THE JOURNAL OF PHYSICAL CHEMISTRY A
A JOURNAL OF THE AMERICAN CHEMICAL SOCIETY

pubs.acs.org/JPCA

Article

Theoretical and Experimental Study of the Spectroscopy and Thermochemistry of $UC^{+/0/-}$

Gabriel F. de Melo, Monica Vasiliu, Gaoxiang Liu, Sandra Ciborowski, Zhaoguo Zhu, Moritz Blankenhorn, Rachel Harris, Chalynette Martinez-Martinez, Maria Dipalo, Kirk A. Peterson, Kit H. Bowen,* and David A. Dixon*

Cite This: *J. Phys. Chem. A* 2022, 126, 9392−9407

Read Online

ACCESS | Metrics & More | Article Recommendations | Supporting Information

ABSTRACT: A combination of high-level *ab initio* calculations and anion photoelectron detachment (PD) measurements is reported for the UC, UC^-, and UC^+ molecules. To better compare the theoretical values with the experimental photoelectron spectrum (PES), a value of 1.493 eV for the adiabatic electron affinity (AEA) of UC was calculated at the Feller−Peterson−Dixon (FPD) level. The lowest vertical detachment energy (VDE) is predicted to be 1.500 eV compared to the experimental value of 1.487 ± 0.035 eV. A shoulder to lower energy in the experimental PD spectrum with the 355 nm laser can be assigned to a combination of low-lying excited states of UC^- and excited vibrational states. The VDEs calculated for the low-lying excited electronic states of UC at the SO-CASPT2 level are consistent with the observed additional electron binding energies at 1.990, 2.112, 2.316, and 3.760 eV. Potential energy curves for the Ω states and the associated spectroscopic properties are also reported. Compared to UN and UN^+, the bond dissociation energy (BDE) of UC (411.3 kJ/mol) is predicted to be considerably lower. The natural bond orbitals (NBO) calculations show that the $UC^{0/+/-}$ molecules have a bond order of 2.5 with their ground-state configuration arising from changes in the oxidation state of the U atom in terms of the 7s orbital occupation: UC ($5f^27s^1$), UC^- ($5f^27s^2$), and UC^+ ($5f^27s^0$). The behavior of the UN and UC sequence of molecules and anions differs from the corresponding sequences for UO and UF.

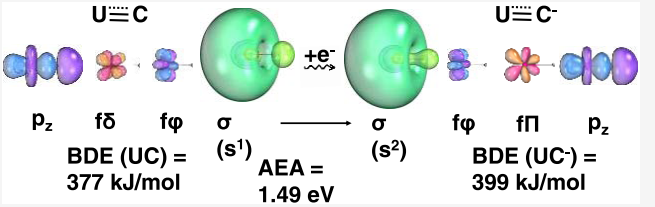

INTRODUCTION

The properties of diatomic actinides provide unique insights into their chemistry and bonding. There is considerable interest in uranium carbides (U_xC_y) and uranium nitrides (U_xN_y) due to their potential to serve as components of alternative nuclear fuels in contrast to the traditional oxide fuels, such as UO_2.[1,2] The nitrides and carbides offer several advantages for the operation of generation IV reactors, especially for gas-cooled fast reactors, due to their enhanced thermophysical properties.[1,3−5] Since some fuels may involve mixing of uranium and plutonium carbides, it is important to obtain additional information about their chemistry to improve performance and safety.

The description of the role of 5f electrons on different actinide−ligand interactions is important to understanding their chemistry, and computational approaches can provide useful information. Although computational studies of uranium monocarbide UC have been reported,[6−11] the properties of its excited states and ions have not been explored extensively. Wang et al.[12,13] collected laser-evaporated carbon-rich U/C alloys in solid argon and neon matrices at 8 K to form U≡C, U≡CH, C≡U≡C, and $U(CC)_2$. The vibrational frequencies were measured, and the fundamental vibration for UC was found at 871.7 cm^{-1} in Ne and at 827.8 cm^{-1} in Ar. Their CASPT2 calculations with spin−orbit coupling predicted a quintet ground state (Ω = 3) with r_e = 1.863 Å and ω_e = 945 cm^{-1}. Pogány et al.[14] performed SO-CASPT2 relativistic calculations with a valence triple-ζ basis set on UC as well for the monocarbides ThC, PuC, and AmC; they predicted the excited states of UC up to ∼13,000 cm^{-1}. A dissociation energy of 402 kJ/mol was predicted for UC (UC → U + C) with ThC (562 kJ/mol) being the most stable molecule of the group and AmC the least stable (221 kJ/mol); the values for NpC (332 kJ/mol) and PuC (365 kJ/mol) were intermediate between the extremes.[14]

In our prior work on $UN^{0/-/+}$,[15] we showed that the ground states of UN ($5f^27s^1$), UN^- ($5f^27s^2$), and UN^+ ($5f^27s^0$) arise from changes in the oxidation state of U in terms of the 7s orbital occupations, and the nature of the ligand is not significantly affected. The U≡N triple bond was found to have mostly f and d characters, so the 7s orbital where the oxidation

Received: October 3, 2022
Revised: November 28, 2022
Published: December 12, 2022

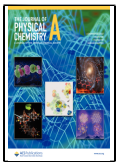

is occurring acts like a spectator orbital. To a first approximation, as UC is isoelectronic to UN^+, we might predict that they have the same ground-state electronic configuration. In contrast, Heaven, Peterson, and co-workers[16] reported a $^3H_4$ ground state for UN^+ from high-level electronic structure calculations, whereas Pogány et al.[14] predicted a ^5H ground state for UC. To better understand the properties of UC and its electronic structure in relation to UN, the current work investigates U-C in more detail based on high-level *ab initio* calculations on UC, UC^-, and UC^+ and photoelectron spectroscopy (PES) of UC^-. Electron affinities (AEA) and vertical detachment energies (VDE) were calculated to aid in the interpretation of the experimental photoelectron spectrum (PES) of UC^-. Comparison with the prior work[15,16] on the isoelectronic U≡N/U≡N^+ molecules is made to provide insights into how the electronic structure varies with the ligand.

EXPERIMENTAL AND COMPUTATIONAL METHODS

Experimental Section. UC^- anions were generated by ablating a depleted uranium rod. The ion source and the photoelectron spectrometer have been described in detail previously.[17] The uranium rod was ablated by the 2nd harmonic of a Nd:YAG laser (532 nm) while rotating and translating. The generated cations, anions, and neutrals were crossed with 20 psi of a 5% C_2H_6 (in He) gas mixture, coming out of a pulsed valve. The particles were then guided through a skimmer into a Wiley−McLaren-type time-of-flight mass spectrometer.

The ions were then mass gated (to only let UC^- anions pass) and crossed with the third or fourth harmonic of a Nd:YAG laser (355 nm, 3.49 eV and 266 nm, 4.66 eV). The kinetic energy of the electrons was then measured with a magnetic bottle energy analyzer (resolution of ∼ 35 meV at 1 eV EKE). The binding energy is calculated with the well-known relation $h\upsilon$ = EBE + EKE, where hυ is the energy of the photon, EKE is the measured kinetic energy, and EBE is the binding energy of the electron. The spectra were calibrated with the known Cu^- spectrum.[18]

Computational Methods. To obtain the potential energy curves for the Ω states, first the complete active space self-consistent field (CASSCF)[19,20] approach was used to represent each lowest spin-free state, ΛS, followed by second-order perturbation theory (CASPT2).[21,22] The atomic basis sets used were the aug-cc-pVnZ (n = D, T, Q) basis sets[23,24] for C and the cc-pVnZ-PP basis sets,[25,26] including a 60-electron small effective core potential optimized in multiconfigurational Dirac−Hartree−Fock calculations, for U. These combined basis sets are denoted as an-PP. These calculations were carried out in the highest Abelian point group available, C_{2v}, for both molecules. Expectation values of L_z^2 were calculated to ensure that both degenerate components of each Λ state were correctly accounted for.

The active space of UC includes four electrons in nine orbitals ($4 \times a_1$, $2 \times b_1$, $2 \times b_2$, $1 \times a_2$ in C_{2v} symmetry) which have dominant $2p_z$ of carbon and 5f, 7s of uranium. For the ions UC^- and UC^+, the same orbitals in the active space were used but now including five and three electrons, respectively. The choice of the (4e/9o) active space used in this work is consistent with the 3 electrons in 8 orbitals used previously for UN, which had also dominant U 5f and 7s characters and yielded results in very good agreement with the photoelectron spectroscopy.[15,16] The state-averaged CASSCF included a total of 11 ΛS quintet states and 18 ΛS triplet states for UC. For UC^-, 46 ΛS states were accounted for, namely, 10 sextets, 17 quartets, and 19 doublets. In the case of UC^+, the ΛS manifold had 19 $^4\Lambda$ and 13 $^2\Lambda$ states. The previous work of Pogány et al.[14] on UC used an active space containing 10 electrons in 16 orbitals where the orbitals up to 5d (U) and 1s (C) were frozen in the CASPT2 calculation. Although their calculations included a lower number of states and larger active space than this work, we performed additional tests including the 5s-6d orbitals of uranium and the 2s of carbon to show that the inclusion of these orbitals in the active space does not have a large impact on the low-lying electronic states. Differences in the energetic order of the low-lying states depending on the active space are discussed in the following section.

On top of the CASSCF zeroth-order wavefunction, second-order multiconfigurational perturbation theory (CASPT2) calculations were carried out using the same active space of the CASSCF. In this step, multiple states are calculated using a Fock operator constructed from a state-averaged density matrix and the zeroth-order Hamiltonians for all states are constructed from the same operator. The frozen-core definition in the CASPT2 included 5s,5p, and 5d orbitals of U and the 1s of C. The lowest possible IPEA[27] shift was used, i.e., a value of 0.28 for all states.

The molecular Ω states arising from the spin−orbit coupling were calculated by applying the state interacting method, as implemented in the MOLPRO (SO-CASPT2)[28−30] suite of programs. In this method, the spin−orbit eigenstates are obtained by diagonalizing $H_{el} + H_{SO}$ in a basis of H_{el} eigenstates. The matrix elements of H_{SO} were constructed using the spin−orbit operator from the U PP. Here, the spin−orbit matrix elements have been calculated throughout at the CASSCF level of the theory using the same basis set as used for the diagonal terms, and the diagonal terms of $H_{el} + H_{SO}$ have been replaced with CASPT2 energies. The latter energies for the 2 components of each molecular state with $\Lambda \neq 0$ were manually averaged when needed to ensure exact degeneracies. After diagonalization of $H_{el} + H_{SO}$, the values of Ω for each molecule were assigned by converting from a Cartesian eigenfunction basis to a spherical basis, and then adding the projection of the spin angular momentum S on the diatomic axis, Σ, to Λ to obtain Ω.[31]

The initial geometry of the multireference calculations was obtained through open-shell calculations for the ground state of $UC^{0/+/-}$ performed with the R/UCCSD(T) approach. In this method, a restricted open-shell Hartree−Fock calculation is carried out followed by a relaxation of the spin constraint at the coupled cluster level.[32−35] These calculations used the third-order Douglas-Kroll-Hess Hamiltonian (DKH3)[36−38] with the aug-cc-pVnZ-DK basis set[23,39] for C and the cc-pwCV*n*Z-DK3 basis set for U.[25,26] The potential energy curves for the diatomics were obtained at the SO-CASPT2/aQ-PP level by computing seven single-point energies distributed around the equilibrium bond length of the ground state ($r-r_e$ = −0.3, −0.2, −0.1, 0.0, +0.1, +0.3, +0.5 Bohr) optimized at the CCSD(T)/awQ-DK level.[40−42]

The electron detachment properties (AEA and VDE) and bond dissociation energies (BDEs) were predicted using the Feller−Peterson−Dixon (FPD)[43−46] composite thermochemistry method. The contributions included in these calculations are defined by

https://doi.org/10.1021/acs.jpca.2c06978
J. Phys. Chem. A 2022, 126, 9392−9407

$$\Delta E_0 = \Delta E_{CBS} + \Delta E_{CV} + \Delta E_{SO} + \Delta E_{Gaunt} + \Delta E_{QED} + \Delta E_T + \Delta E_Q + \Delta E_{ZPE}$$

The ΔE_{CBS} is the CCSD(T) energy value at the CBS limit using awn-DK basis set for n = D, T, and Q, ΔE_{CV} represents the contribution of the additional correlation due to the valence and outer core electrons, and ΔE_{ZPE} are the zero-point energies calculated as 0.5 ω_e − 0.25 $\omega_e x_e$ with frequencies obtained from fitting the CCSD(T)/awQ-DK curve (not included for the VDE calculations).[47] The spin−orbit (ΔE_{SO}) contributions were taken from the SO-CASPT2 energy corrections using the aQ-DK basis set. The Gaunt term (ΔE_{Gaunt}), which accounts for spin−other−orbit coupling, was obtained by the energy difference between Dirac−Hartree−Fock calculations with the four-component Dirac−Coulomb (DC) and the Dirac−Coulomb−Gaunt (DCG) Hamiltonians using fully uncontracted basis sets, cc-pVDZ-DK3 on U and aug-cc-pVDZ on C. These calculations were carried out using the DIRAC program.[48] Effects due to the leading term of quantum electrodynamics (ΔE_{QED}), the Lamb shift, were obtained from the local model potential approach proposed by Pyykkö and Zhao[49] for the self-energy term, as well as a fit to the Uehling potential for the vacuum polarization.[26] These calculations were done at the frozen-core DK3-CCSD(T) level with the awD-DK basis sets. Higher-order correlation effects were calculated using the DKH3 Hamiltonian with the MRCC[50,51] package connected to MOLPRO, where ΔE_T = CCSDT − CCSD(T) with the aT-DK basis sets[52,53] and ΔE_Q = CCSDT(Q) − CSSDT with the aD-DK basis sets.[54]

A bonding analysis of the $UC^{0/+/-}$ species was made through the natural population analysis (NPA) results based on the natural bond orbitals (NBOs)[55,56] using NBO7[57,58] with the MOLPRO program package at the aD-DK level.

RESULTS AND DISCUSSION

The observed photoelectron spectrum (PES) of UC^- obtained using the 3rd and 4th harmonic is presented in Figure 1. Numerous peaks are present in the spectra. Specific EBEs were assigned to peaks located at 1.487 ± 0.035, 1.990, 2.112, 2.316, and 3.760 eV. The lowest energy, intense transition (the first large EBE peak) corresponds to the vertical detachment energy (VDE) from the UC^- ground state to the ground state of its neutral counterpart where the Franck-Condon overlap between the wavefunction of the ground state of the anion and that of the neutral is maximal. Transitions from excited electronic and excited vibrational states of the anion will occur at energies below the VDE from the ground state anion and the shoulder from 1.1 to 1.3 eV in the 355 nm (3.49 eV) spectrum can be accounted for by such transitions as discussed below.

Electronic Structure of UC^-. From the SO-CASPT2 calculations, the equilibrium excitation energies for the low-lying states of UC^- are given together with their corresponding ΛS compositions in Table 1. The spectroscopic constants calculated for the potential energy curves (Figure 2) of the states with energies lower than ∼1.0 eV are collected in Table 2. A total of 83 states was obtained within ∼2.6 eV, with 61 states below ∼2.0 eV. This number is slightly larger than the 50 states obtained for UN within ∼2.0 eV.[15] The ground state of UC^-, Ω = 2.5, is well described by the $^4\Gamma$ state with small contributions from the $^4\Phi$ and $^2\Phi$ states. At the SO-CASPT2 level, the values of r_e = 1.886 Å and ω_e = 957.3 cm^{-1} for UC^- are in reasonable agreement with the values of r_e = 1.891 Å and ω_e = 934.6 cm^{-1} calculated at the CCSD(T)/awQ-DK level. Note that the higher-energy states (Figure 2) have more anharmonic character due in part to mixing with other states.

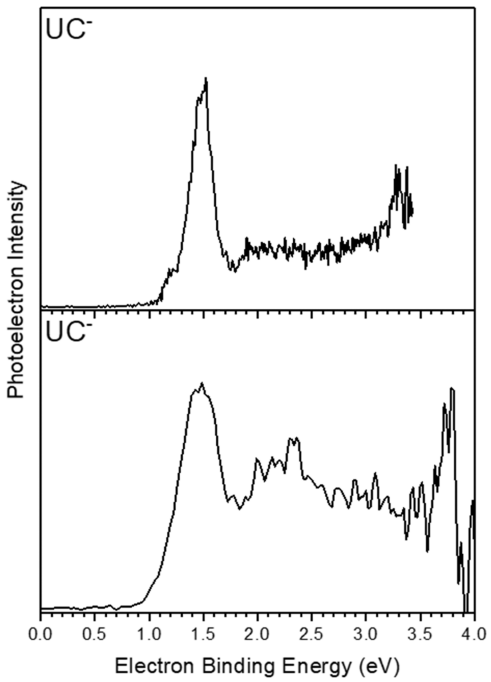

Figure 1. Photoelectron spectra of UC^- obtained using the third (355 nm, 3.49 eV) (top) and fourth harmonic (266 nm, 4.66 eV) (bottom) of a Nd:YAG laser.

Most of the excited spin−orbit states of UC^- have high multireference character, with compositions involving several ΛS states. The first excited state, Ω = 3.5, also with a dominant $^4\Gamma$ state character, is only 0.079 eV (637 cm^{-1}) higher than the ground state. The isoelectronic UN molecule ($^4H_{7/2}$) has all of its unpaired electrons on the U in a $5f^27s^1$ configuration. In contrast, the UC^- electronic configuration has two unpaired electrons in a $5f^2$ configuration on the U and the other unpaired electron in a U-C σ bond with approximately equal contributions from the $2p_z$ on C and a mix of 5f and 6d on the U. This leads to a different ground state for the molecular anion and to a different type of character on the U. An ionic model of $U^{3+}N^{3-}$ provides a reasonable description of UN.[15] Applying such an ionic model $U^{3+}C^{4-}$ to predict the low-lying states of UC^- would result in a $5f^3$ (U) ground-state configuration, which was not predicted by our calculations. Inclusion of spin−orbit effects lowers the energy of the ground state relative to the ΛS state by 5019 cm^{-1} (0.622 eV).

Electronic Structure of UC. For neutral UC, the low-lying quintet and triplet states are displayed in Table 3 with the corresponding spectroscopic constants shown in Table 4 for states up to ∼1.0 eV. UC has an Ω = 3 ground state that is reasonably well described by the pure-spin ^5H state. In addition to the two unpaired 5f (fφ fδ) electrons on U and the singly occupied U-C σ bond found for UC^-, the 7s (U) orbital is now singly occupied. The electronic configuration of the U in UC is the same as that of the U in UN with an atomic $5f^27s^1$ electronic configuration. Calculations performed on UCH (σ fδ fφ) at the SO-CASPT2/aQ-PP level (adding one electron on the ligand but keeping the U configuration unchanged) confirmed that the resulting electronic states are the same as

https://doi.org/10.1021/acs.jpca.2c06978
J. Phys. Chem. A 2022, 126, 9392−9407

Table 1. Low-Lying States of UC^- at the CASPT2/aQ-PP + SO Level

state	Ω	ΔE (eV)	ΛS composition
$^4\Gamma_{5/2}$	2.5	0.000	81% $^4\Gamma$ + 10% $^4\Phi$ + 7% $^2\Phi$
$^4\Gamma_{7/2}$	3.5	0.079	40% $^4\Gamma$ + 32% $^2\Gamma$ + 13% $^4\Phi$ + 9% $^2\Phi$ + 6% $^2\Phi$
$^2\Phi_{5/2}$	2.5	0.164	42% $^2\Phi$ + 18% $^4\Delta$ + 17% $^4\Phi$ + 16% $^2\Delta$ + 5% $^2\Delta$
$^4\Phi_{3/2}$	1.5	0.240	57% $^4\Phi$ + 27% $^4\Delta$ + 16% $^2\Delta$
$^4\Gamma_{9/2}$	4.5	0.560	72% $^4\Gamma$ + 17% $^2\Gamma$ + 10% $^4\Phi$
$^4\Gamma_{7/2}$	3.5	0.564	50% $^4\Gamma$ + 28% $^2\Phi$ + 20% $^2\Gamma$
$^4\Delta_{7/2}$	3.5	0.594	100% $^4\Delta$
$^2\Phi_{5/2}$	2.5	0.743	38% $^2\Phi$ + 29% $^4\Delta$ + 18% $^4\Phi$ + 9% $^4\Gamma$ + 3% $^2\Delta$
$^4\Delta_{3/2}$	1.5	0.764	52% $^4\Delta$ + 26% $^2\Delta$ + 20% $^4\Phi$
$^4\Delta_{5/2}$	2.5	0.785	43% $^4\Delta$ + 31% $^4\Phi$ + 19% $^2\Gamma$ + 5% $^2\Phi$
$^6I_{7/2}$	3.5	0.804	86% ^6I + 8% ^6H + 6% ^4H
$^4\Phi_{5/2}$	2.5	0.914	45% $^4\Phi$ + 21% $^4\Delta$ + 19% $^2\Delta$ + 5% $^4\Gamma$ + 4% $^2\Phi$ + 3% $^2\Delta$
$^4\Sigma_{1/2}^-$	0.5	0.942	78% $^4\Sigma^-$ + 12% $^4\Pi$ + 8% $^2\Pi$ + 2% $^2\Sigma^-$
$^4\Delta_{5/2}$	2.5	0.976	35% $^4\Delta$ + 22% $^2\Phi$ + 22% $^2\Gamma$ + 12% $^2\Phi$ + 8% $^4\Phi$
$^6I_{9/2}$	4.5	0.982	53% ^6I + 27% ^4I + 10% ^6H + 5% ^4H + 3% ^2H
$^4\Sigma_{3/2}^-$	1.5	1.024	84% $^4\Sigma^-$ + 10% $^2\Pi$ + 5% $^4\Pi$
$^4\Gamma_{11/2}$	5.5	1.048	100% $^4\Gamma$
$^2\Delta_{3/2}$	1.5	1.068	43% $^2\Delta$ + 29% $^2\Delta$ + 22% $^4\Phi$ + 4% $^4\Delta$
$^2\Delta_{5/2}$	2.5	1.073	45% $^2\Delta$ + 38% $^2\Phi$ + 9% $^4\Delta$ + 4% $^4\Gamma$ + 3% $^2\Phi$
$^2\Phi_{7/2}$	3.5	1.108	35% $^2\Phi$ + 31% $^4\Phi$ + 20% $^2\Gamma$ + 7% $^4\Gamma$ + 3% $^2\Gamma$ + 3% $^2\Phi$
$^4\Phi_{9/2}$	4.5	1.119	72% $^4\Phi$ + 21% $^2\Gamma$ + 4% $^2\Gamma$ + 3% $^4\Gamma$
$^6H_{5/2}$	2.5	1.137	87% ^6H + 12% $^6\Gamma$
$^2\Gamma_{9/2}$	4.5	1.192	75% $^2\Gamma$ + 23% $^4\Gamma$
$^6I_{11/2}$	5.5	1.215	60% ^6I + 16% ^6H + 17% ^4I + 5% ^4H
$^2\Sigma_{1/2}^-$	0.5	1.217	63% $^2\Sigma^-$ + 25% $^2\Pi$ + 7% $^4\Sigma^-$ + 4% $^4\Pi$
$^6H_{7/2}$	3.5	1.232	57% ^6H + 14% $^6\Gamma$ + 15% ^4H + 9% ^4H + 4% ^6I
$^4I_{9/2}$	4.5	1.252	50% ^4I + 28% ^6I + 7% ^6H + 7% ^2H + 6% ^4H
$^6H_{9/2}$	4.5	1.385	45% ^6H + 18% $^6\Gamma$ + 15% ^4H + 10% ^6I + 10% ^4H
$^6\Gamma_{3/2}$	1.5	1.390	100% $^6\Gamma$
$^2\Delta_{3/2}$	1.5	1.442	40% $^2\Delta$ + 31% $^2\Delta$ + 15% $^4\Delta$ + 11% $^2\Pi$ + 3% $^4\Pi$
$^4H_{7/2}$	3.5	1.456	76% ^4H + 11% ^4H + 7% $^6\Gamma$
$^2\Pi_{1/2}$	0.5	1.461	63% $^2\Pi$ + 21% $^2\Sigma^-$ + 13% $^4\Pi$
$^6I_{13/2}$	6.5	1.468	66% ^6I + 20% ^6H + 10% ^4I + 3% ^4H
$^2\Delta_{5/2}$	2.5	1.516	57% $^2\Delta$ + 20% $^4\Delta$ + 13% $^2\Phi$ + 5% $^4\Pi$ + 2% $^2\Phi$
$^4I_{11/2}$	5.5	1.524	46% ^4I + 20% ^6I + 17% ^4H + 11% ^2I + 3% ^6H
$^6\Delta_{1/2}$	0.5	1.532	74% $^6\Delta$ + 24% $^6\Pi$
$^6\Delta_{1/2}$	0.5	1.565	54% $^6\Delta$ + 39% $^6\Pi$ + 2% $^4\Pi$
$^6H_{11/2}$	5.5	1.592	41% ^6H + 26% $^6\Gamma$ + 15% ^4H + 11% ^6I + 3% ^4H
$^6\Gamma_{5/2}$	2.5	1.610	87% $^6\Gamma$ + 13% ^6H
$^6\Delta_{3/2}$	1.5	1.635	39% $^6\Delta$ + 38% $^6\Pi$ +12% $^2\Pi$ + 5% $^4\Pi$ + 3% $^4\Pi$
$^2\Pi_{3/2}$	1.5	1.649	67% $^2\Pi$ + 8% $^4\Sigma^-$ + 7% $^6\Pi$ + 6% $^6\Delta$ + 6% $^2\Delta$ + 4% $^2\Delta$
$^2\Phi_{5/2}$	2.5	1.684	66% $^2\Phi$ + 19% $^4\Delta$ + 11% $^4\Phi$
$^4H_{7/2}$	3.5	1.714	69% ^4H + 8% ^6I + 6% $^6\Gamma$ + 6% ^6H + 5% $^2\Gamma$ + 4% ^4H
$^2\Phi_{5/2}$	2.5	1.741	36% $^2\Phi$ + 21% $^2\Delta$ + 18% $^2\Delta$ + 8% $^4\Phi$ + 5% $^4\Pi$ + 5% $^2\Phi$
$^4\Pi_{1/2}$	0.5	1.750	33% $^4\Pi$ + 25% $^6\Pi$ + 14% $^6\Delta$ + 11% $^4\Pi$ + 7% $^2\Sigma^-$ + 7% $^4\Sigma^-$
$^4H_{9/2}$	4.5	1.756	56% ^4H + 15% ^4H + 15% ^4I + 11% $^6\Gamma$
$^6\Delta_{5/2}$	2.5	1.764	43% $^6\Delta$ + 42% $^6\Pi$ + 6% $^4\Pi$ + 3% $^2\Delta$ + 3% $^4\Pi$
$^6I_{15/2}$	7.5	1.772	80% ^6I + 16% ^6H + 4% ^4I
$^6\Pi_{3/2}$	1.5	1.779	100% $^6\Pi$
$^4\Pi_{1/2}$	0.5	1.814	41% $^4\Pi$ + 22% $^6\Pi$ + 13% $^4\Pi$ + 13% $^6\Delta$ + 6%
$^2\Gamma_{7/2}$	3.5	1.823	74% $^2\Gamma$ + 8% $^2\Phi$ + 5% ^4H + 5% $^4\Phi$ + 3% $^4\Gamma$ + 3% $^2\Gamma$
$^6\Gamma_{7/2}$	3.5	1.825	73% $^6\Gamma$ + 24% ^6H + 2% ^4H
$^2H_{9/2}$	4.5	1.829	31% ^2H + 24% ^4H + 11% ^4H + 11% $^2\Gamma$ + 7% ^6H + 7% $^6\Gamma$
$^4\Pi_{1/2}$	0.5	1.832	33% $^4\Pi$ + 21% $^6\Delta$ + 19% $^6\Pi$ + 18% $^4\Pi$ + 5% $^4\Sigma^-$
$^6\Gamma_{13/2}$	6.5	1.881	24% $^6\Gamma$ + 24% ^6I + 23% ^6H + 11% ^4H + 12% ^4H + 3% $^4\Pi$
$^2\Gamma_{9/2}$	4.5	1.897	67% $^2\Gamma$ + 13% $^4\Phi$ + 6% ^2H + 5% ^4H + 3% $^2\Gamma$
$^4I_{13/2}$	6.5	1.901	49% ^4I + 18% ^4H + 12% ^6H + 11% $^6\Gamma$ + 6% ^2I

https://doi.org/10.1021/acs.jpca.2c06978
J. Phys. Chem. A 2022, 126, 9392−9407

Table 1. continued

state	Ω	ΔE (eV)	ΛS composition
$^4\Pi_{3/2}$	1.5	1.906	67% $^4\Pi$ + 20% $^6\Delta$ + 4% $^4\Sigma^-$ + 4% $^4\Pi$
$^4\Pi_{1/2}$	0.5	1.913	53% $^4\Pi$ + 16% $^4\Pi$ + 15% $^6\Pi$ + 9% $^6\Delta$ + 7% $^4\Sigma^-$
$^6\Delta_{7/2}$	3.5	1.918	62% $^6\Delta$ + 38% $^6\Pi$
$^2I_{11/2}$	5.5	1.995	80% ^2I + 5% $^4\Sigma^-$ + 3% ^2H + 3% ^6I
$^4\Pi_{5/2}$	2.5	2.003	80% $^4\Pi$ + 11% $^6\Delta$ + 7% $^2\Delta$
$^4\Pi_{3/2}$	1.5	2.020	29% $^4\Pi$ + 27% $^6\Delta$ + 21% $^6\Pi$ + 21% $^4\Pi$
$^6\Gamma_{9/2}$	4.5	2.029	58% $^6\Gamma$ + 28% ^6H + 9% ^4H
$^6\Gamma_{11/2}$	5.5	2.038	31% ^4H + 29% $^6\Gamma$ + 15% ^4I + 12% ^6H + 12% ^4H
$^6\Delta_{5/2}$	2.5	2.097	37% $^6\Delta$ + 33% $^4\Pi$ + 23% $^6\Pi$ + 7% $^4\Pi$
$^6I_{17/2}$	8.5	2.120	100% ^6I
$^6\Delta_{9/2}$	4.5	2.146	100% $^6\Delta$
$^4H_{11/2}$	5.5	2.149	32% ^4H + 31% ^4H + 18% ^6H + 6% ^2I + 6% ^2H + 5% ^6I
$^2H_{9/2}$	4.5	2.159	50% ^2H + 40% ^4H + 5% ^4I + 2% $^6\Gamma$ + 2% ^6I
$^6\Gamma_{13/2}$	6.5	2.197	42% $^6\Gamma$ + 32% ^6H + 8% ^4H + 7% ^4H + 7% $^6\Delta$ + 3% ^6I
$^6H_{15/2}$	7.5	2.237	72% ^6H + 15% ^6I + 12% ^6H
$^6\Gamma_{11/2}$	5.5	2.244	42% $^6\Gamma$ + 25% ^4H + 11% ^4H + 10% ^6H + 6% ^2H + 5% ^4I
$^6\Pi_{7/2}$	3.5	2.257	62% $^6\Pi$ + 38% $^6\Delta$
$^4\Pi_{1/2}$	0.5	2.306	72% $^4\Pi$ + 23% $^6\Pi$ + 5% $^6\Delta$
$^4H_{13/2}$	6.5	2.356	37% ^4H + 30% ^4I + 11% ^6H + 11% ^2I + 6% ^4H + 5% ^6I
$^4I_{15/2}$	7.5	2.399	95% ^4I + 5% ^6I
$^4\Pi_{1/2}$	0.5	2.409	64% $^4\Pi$ + 30% $^6\Pi$ + 6% $^6\Delta$
$^4\Pi_{5/2}$	2.5	2.434	60% $^4\Pi$ + 33% $^6\Pi$ + 7% $^6\Delta$
$^4\Pi_{3/2}$	1.5	2.443	60% $^4\Pi$ + 33% $^6\Pi$ + 7% $^6\Delta$
$^4H_{13/2}$	6.5	2.517	64% ^4H + 20% $^6\Gamma$ + 9% ^4H + 5% ^2I
$^2I_{13/2}$	6.5	2.617	78% ^2I + 12% ^4H + 9% ^4H
$^2H_{11/2}$	5.5	2.644	81% ^2H + 15% ^4H + 2% ^4I

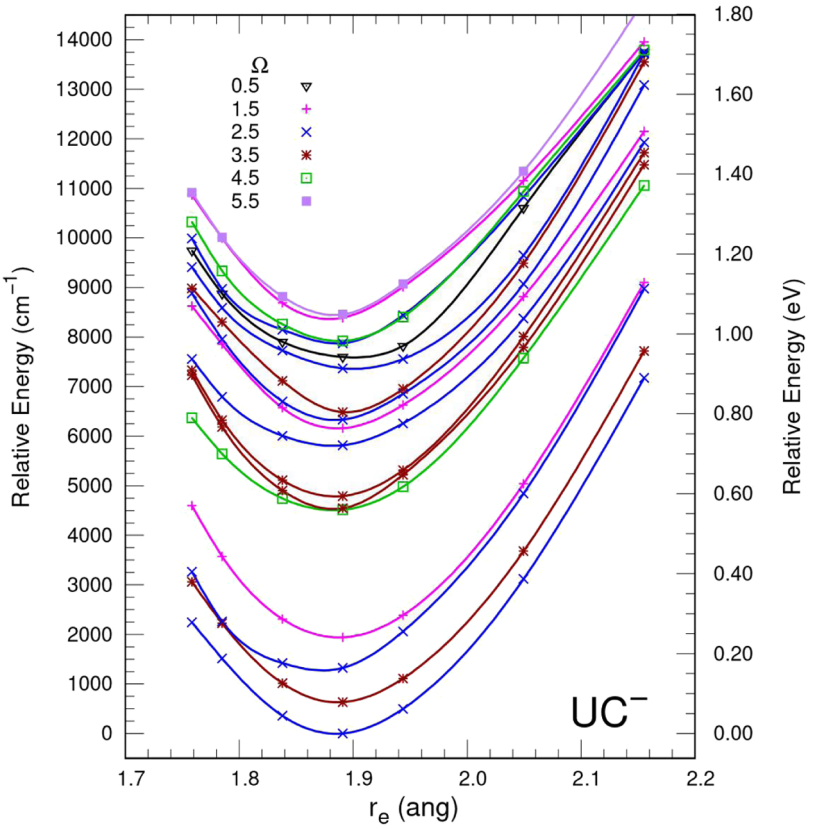

Figure 2. SO-CASPT2/aQ-PP potential energy curves for the low-lying Ω states of UC^-.

https://doi.org/10.1021/acs.jpca.2c06978
J. Phys. Chem. A 2022, 126, 9392−9407

Table 2. SO-CASPT2/aQ-PP Spectroscopic Parameters for Selected Low-Lying Ω States of UC^-

Ω state	T_e (cm^{-1})	r_e (Å)	ω_e (cm^{-1})	$\omega_e x_e$ (cm^{-1})	B_e (cm^{-1})
$^4\Gamma_{5/2}$	0	1.886	957.3	11.0	0.415
$^4\Gamma_{7/2}$	637	1.895	927.2	8.9	0.411
$^2\Phi_{5/2}$	1323	1.871	937.9	14.7	0.421
$^4\Phi_{3/2}$	1936	1.888	936.4	8.8	0.414
$^4\Gamma_{9/2}$	4517	1.882	857.5	8.5	0.417
$^4\Gamma_{7/2}$	4549	1.887	926.5	1.3	0.415
$^4\Delta_{7/2}$	4791	1.885	904.6	1.2	0.415
$^2\Phi_{5/2}$	5993	1.880	819.3	8.9	0.417
$^4\Delta_{3/2}$	6162	1.892	879.4	3.6	0.412
$^4\Delta_{5/2}$	6331	1.885	977.4	11.5	0.415
$^6I_{7/2}$	6485	1.888	969.0	6.3	0.414
$^4\Phi_{5/2}$	7372	1.900	763.1	2.3	0.409
$^4\Sigma_{1/2}^-$	7598	1.887	875.7	10.7	0.414
$^4\Delta_{5/2}$	7872	1.878	988.4	14.6	0.418
$^6I_{9/2}$	7920	1.885	949.5	23.6	0.415

obtained previously for UN.[15] The energetic order of the Ω states of UCH and UN can be seen in Table S2.

The first excited state of UC, $^5H_4$, is a spin−orbit component of the ground state that is only 0.050 eV (430 cm^{-1}) higher than the ground state. The $^5H_4$ state is 0.143 eV lower than the $^5\Gamma_2$ state. In contrast, Pogány et al.[14] predicted the first excited state to be $^5\Gamma_2$, located 0.234 eV (1888 cm^{-1}) above the ground state and the $^5H_4$ state to be at 0.262 eV (2114 cm^{-1}). Their calculation used a larger active space (10 electrons/16 orbitals) but included fewer states than the current work. As discussed above, the inclusion of more active orbitals did not have a large impact in the low-lying structure of states. We carried out calculations correlating all of the 5s-7s electrons of U and the 2s-2p of C at the SO-CASPT2 level but the energetic ordering of the first two excited states remained the same (Table S3). At the SO-CASPT2/CBS level, the correlation of core electrons increases the excitation energy of the $^5\Gamma_2$ state to 2110 cm^{-1} (Table S4) compared to the valence-only calculation (1606 cm^{-1}) at the same level, both in agreement with the value obtained at the CCSD(T)/CBS level (1733 cm^{-1}); these energies for the $^5\Gamma_2$ state are consistent with the prior work for this state.[14] Thus, we do not know exactly what causes the difference in state orderings for the first two excited states but it could be due to the inclusion of a larger number of electronic states which might place the $^5H_4$ lower in energy than the $^5\Gamma_2$ state.

The values of r_e = 1.854 Å and ω_e = 949.6 cm^{-1} obtained for UC at the SO-CASPT2/aug-pwCVQZ level are similar to those obtained in the current work at the CCSD(T)/aug-pwCVQZ level (r_e =1.8699 Å, ω_e = 922.0 cm^{-1}, $\omega_e x_e$ = 3.5 cm^{-1}) and those reported by Wang et al.[13] (r_e = 1.863 Å and ω_e = 945 cm^{-1}) at the SO-CASPT2 level using a 10 electron/12 orbital active space with a valence triple-ζ basis set and by Pogány et al.[14] at the SO-CASPT2 level (10e/16o) with a valence triple-ζ basis set (r_e = 1.870 Å and ω_e = 928 cm^{-1}). The r_e of UC is longer than that obtained for UN (r_e = 1.768 Å) and UN^+ (r_e = 1.731 Å) at the SO-CASPT2 level.[15] Basis set convergence of the spectroscopic properties of the ^5H and $^5\Gamma$ states at the CCSD(T) level are shown in Table S5. The value of $\omega_e x_e$ is small for all states, on the order of or less than 10 cm^{-1}, so this will not dramatically affect the frequencies. The experimental value for the fundamental vibrational transition in UC is 871.7 cm^{-1} in a Ne matrix and 827.8 cm^{-1} in an Ar matrix. These values show that there is a large matrix shift in UC. The difference between the gas phase value of ν = 920 cm^{-1} at the CCSD(T) level and the Ne value of 872 cm^{-1} suggests that the Ne matrix is strongly interacting with UC. The argument[13] presented for the large matrix shift between Ne and Ar being due to changing electronic states from the quintet to a triplet is not consistent with our SO-CASPT2 value of ω_e = 968 cm^{-1} for the $^3H_4$ which is 0.27 eV above the ground state. Although the $^3\Gamma_3$ state has ω_e = 854 cm^{-1}, it is 0.63 eV above the ground state. There is a second $^3\Gamma_3$ state with ω_e = 811 cm^{-1}, but it is 0.94 eV higher in energy. Most of the remaining excited states below ∼1.6 eV have predicted vibrational transitions above 900 cm^{-1} except for the $^5\Pi_1$ with ω_e = 890 cm^{-1} and the $^5H_5$ with ω_e = 872 cm^{-1}; these states are 0.24 and 0.76 eV above the ground state, respectively. Adding one electron to UC to form the anion decreases the bond length by 0.032 Å and increases ω_e by 7.7 cm^{-1}.

We predicted 59 states with energies below ∼1.65 eV for UC. Compared to UN^+ ($5f^2$) where 16 states were reported within 1.22 eV, UC has a considerably denser manifold of states in this range with 39 states predicted. Similar to UC^-, the excited states of UC are strongly mixed although the low-lying states have dominant quintet character. The first triplet state is predicted to be 0.634 eV higher than the ground state. A global picture of the Ω states is shown in Figure 3. Note that above ∼8000 cm^{-1} there are some interactions between the states, leading to slightly distorted potential curves. For UC, the inclusion of the spin−orbit coupling lowers the ground state energy by 0.639 eV (5151 cm^{-1}).

Electron Detachment Energies. We now discuss the electron detachment energies of UC^-. To interpret the PES spectrum, an accurate adiabatic electron affinity (AEA) is needed. The Feller−Peterson−Dixon (FPD) approach was used to calculate the AEA. Table 5 collects the FPD components obtained with DK basis sets at the CCSD(T) level. The T_1 diagnostics of the three molecules ranged from 0.03 to 0.05 for the ground states. Considering the small doubles amplitudes, high-quality coupled cluster results should be expected for these states. The AEA was obtained as the relative energy of the ground states of UC and UC^-. The final AEA (UC ($^5H_3$) + e^- → UC^- ($^4\Gamma_{5/2}$)) was calculated to be 1.493 eV (144.1 kJ/mol) which is slightly higher than the EA of UN (1.402 eV, 135.3 kJ/mol) at the same level.[15] Most of the FPD contributions beyond CCSD(T) are quite small. The difference between the EA(CBS) and the final FPD value is 0.018 eV, because of the similar contributions of different signs. The spin−orbit effects decrease the EA by 0.016 eV, whereas the Gaunt term increases it by only 0.005 eV. The higher-correlation contributions, CCSDT and CCSDT(Q), lead to a decrease of −0.02 eV. The vertical detachment energy (VDE) was calculated at the UC^- ($^4\Gamma_{5/2}$) equilibrium geometry and includes all of the FPD components with exception of the ΔE_{ZPE}. The final VDE is 1.500 eV, which is 0.007 eV (0.68 kJ/mol) higher than the EA.

The predicted EA and VDE are consistent with the peaks observed in the experimental PES (Figure 1). The first large maximum, located at 1.487 eV, is broad and ranges from ∼1.0 to ∼1.7 eV. There are three states in this interval including the ground state $^5H_3$ as shown in Table 6. Following that, we note numerous peaks with lower intensity than the first one. Thus, in this region, the specific assignments of the excited UC states

https://doi.org/10.1021/acs.jpca.2c06978
J. Phys. Chem. A 2022, 126, 9392−9407

Table 3. Low-Lying States of UC at the CASPT2/aQ-PP + SO Level

state	Ω	Δ*E* (eV)	ΛS composition
$^5H_3$	3	0.000	80% ^5H + 16% $^5\Gamma$ + 2% $^5\Phi$
$^5H_4$	4	0.050	50% ^5H + 23% ^3H + 17% $^5\Gamma$
$^5\Gamma_2$	2	0.193	58% $^5\Gamma$ + 26% $^5\Phi$ + 11% $^5\Delta$ + 4% $^5\Pi$
$^5\Pi_1$	1	0.236	35% $^5\Pi$ + 30% $^5\Delta$ + 16% $^5\Phi$ + 18% $^5\Sigma^-$
$^5\Phi_3$	3	0.238	25% $^5\Phi$ + 19% $^5\Gamma$ + 15% $^5\Delta$ + 14% $^3\Gamma$ + 10% ^5H + 8% $^3\Phi$
$^5\Pi_0$	0	0.248	48% $^5\Pi$ + 32% $^5\Sigma^-$ + 15% $^5\Delta$
$^5\Pi_2$	2	0.270	23% $^5\Pi$ + 22% $^5\Gamma$ + 22% $^5\Delta$ + 11% $^3\Phi$ + 10% $^3\Delta$ + 9% $^5\Sigma^-$
$^3H_4$	4	0.271	86% $^3\Delta$ + 5% $^3\Gamma$ + 4% ^3H + 4% $^3\Gamma$
$^5H_5$	5	0.278	46% ^5H + 27% ^3H + 18% $^5\Gamma$
$^5\Phi_1$	1	0.349	33% $^5\Phi$ + 18% $^5\Sigma^-$ + 19% $^5\Pi$ +10% $^3\Pi$ + 5% $^3\Sigma^-$ + 5% $^3\Delta$
$^5\Delta_0$	0	0.358	52% $^5\Delta$ + 30% $^5\Pi$ + 10% $^3\Sigma^-$ + 8% $^3\Pi$
$^5\Phi_4$	4	0.459	26% $^5\Phi$ + 19% ^5H + 17% $^5\Gamma$ + 13% $^3\Gamma$ + 9% $^5\Delta$ + 9% $^3\Phi$
$^5\Gamma_3$	3	0.465	31% $^5\Gamma$ + 18% $^5\Delta$ + 17% $^5\Phi$ + 13% $^3\Delta$ + 9% $^3\Phi$ + 6% ^5H
$^5\Sigma_2^-$	2	0.536	29% $^5\Sigma^-$ + 23% $^5\Phi$ + 13% $^3\Pi$ + 10% $^5\Pi$ + 9% $^3\Phi$ +8% $^5\Gamma$
$^5\Pi_1$	1	0.560	44% $^5\Pi$ + 27% $^5\Phi$ + 11% $^3\Sigma^-$ + 9% $^3\Delta$ + 6% $^5\Delta$
$^5\Delta_0$	0	0.579	60% $^5\Delta$ + 18% $^5\Sigma^-$ + 20% $^3\Pi$
$^3\Gamma_3$	3	0.634	47% $^3\Gamma$ + 40% $^3\Gamma$ + 3% $^3\Phi$ + 3% $^5\Pi$ + 3% $^5\Delta$
$^5H_6$	6	0.639	57% ^5H + 28% ^3H + 15% $^5\Gamma$
$^3\Delta_1$	1	0.713	38% $^3\Delta$ + 25% $^3\Pi$ + 11% $^3\Delta$ + 11% $^5\Pi$ + 10% $^5\Phi$
$^3H_4$	4	0.722	61% ^3H + 21% ^5H + 6% $^5\Gamma$ + 5% $^3\Gamma$
$^5H_5$	5	0.765	26% ^5H + 25% $^5\Gamma$ + 23% $^5\Phi$ + 20% $^3\Gamma$ + 5% $^3\Gamma$
$^3\Pi_0$	0	0.780	44% $^3\Pi$ + 29% $^5\Pi$ + 18% $^3\Sigma^-$ + 9% $^3\Sigma^-$
$^5\Gamma_4$	4	0.802	33% $^5\Gamma$ + 30% $^5\Delta$ + 23% $^3\Phi$ + 5% ^5H + 4% $^5\Phi$
$^3\Phi_2$	2	0.830	25% $^3\Phi$ + 19% $^3\Delta$ + 18% $^3\Pi$ + 13% $^5\Delta$ + 11% $^5\Pi$ + 8% $^5\Phi$
$^5\Phi_3$	3	0.832	28% $^5\Phi$ + 27% $^5\Pi$ + 14% $^5\Gamma$ + 11% $^3\Delta$ + 11% $^3\Phi$ + 5% $^5\Delta$
$^3H_5$	5	0.862	85% ^3H + 8% $^3\Gamma$
$^3\Delta_2$	2	0.868	36% $^3\Delta$ + 26% $^5\Sigma^-$ + 19% $^5\Phi$ + 9% $^3\Phi$ + 8% $^5\Gamma$
$^5\Delta_1$	1	0.869	25% $^5\Delta$ + 24% $^5\Sigma^-$ + 19% $^3\Delta$ + 15% $^3\Sigma^-$ + 12% $^5\Phi$
$^5\Delta_0$	0	0.873	41% $^5\Delta$ + 40% $^3\Sigma^-$ + 16% $^5\Pi$
$^3\Gamma_3$	3	0.941	39% $^3\Gamma$ + 20% $^3\Phi$ + 15% $^3\Gamma$ + 10% $^5\Phi$ + 7% $^5\Delta$ + 7% $^3\Delta$
$^3\Delta_1$	1	0.968	48% $^3\Delta$ + 17% $^3\Pi$ + 16% $^3\Sigma^-$ + 13% $^3\Sigma^-$ + 4% $^5\Pi$
$^3H_5$	5	1.050	58% ^3H + 19% ^5H + 11% $^5\Gamma$ + 4% $^3\Gamma$ + 3% $^5\Phi$
$^3\Delta_2$	2	1.112	54% $^3\Delta$ + 21% $^3\Phi$ + 11% $^5\Sigma^-$ + 7% $^5\Delta$
$^3\Gamma_4$	4	1.112	49% $^3\Gamma$ + 14% $^3\Gamma$ + 10% $^5\Delta$ + 10% $^3\Phi$ + 7% $^5\Phi$ + 4% ^3H
$^3\Sigma_1^-$	1	1.194	56% $^3\Sigma^-$ + 16% $^3\Delta$ + 9% $^3\Delta$ + 7% $^3\Delta$ + 4% ^3H
$^3\Delta_3$	3	1.206	30% $^3\Delta$ + 22% $^3\Gamma$ + 14% $^3\Phi$ + 9% $^3\Gamma$ + 9% $^5\Gamma$ + 9% $^5\Pi$
$^5H_7$	7	1.209	100% ^5H
$^3\Sigma_0^-$	0	1.218	80% $^3\Sigma^-$ + 13% $^5\Pi$ + 4% $^3\Pi$
$^3\Pi_0$	0	1.219	79% $^3\Pi$ + 12% $^5\Delta$ + 9% $^5\Sigma^-$
$^3\Gamma_4$	4	1.237	69% $^3\Gamma$ + 11% $^3\Phi$ + 5% $^5\Phi$ + 4% ^3H + 4% $^5\Gamma$
$^3\Pi_2$	2	1.264	34% $^3\Pi$ + 25% $^3\Delta$ + 16% $^3\Phi$ + 8% $^5\Pi$ + 7% $^5\Phi$ + 6% $^3\Delta$
$^3\Sigma_1^-$	1	1.267	28% $^3\Sigma^-$ + 23% $^3\Delta$ + 22% $^3\Sigma^-$ + 20% $^5\Pi$
$^3\Delta_3$	3	1.275	88% $^3\Delta$ + 12% $^5\Pi$
$^5\Gamma_6$	6	1.301	60% $^5\Gamma$ + 33% ^5H + 7% ^3H
$^5\Phi_5$	5	1.384	54% $^5\Phi$ + 40% $^5\Gamma$ + 4% ^5H
$^3H_6$	6	1.396	63% ^3H + 26% $^5\Gamma$ + 19% ^5H
$^5\Pi_0$	0	1.400	50% $^5\Pi$ + 41% $^5\Sigma^-$ + 8% $^5\Delta$
$^5\Pi_1$	1	1.415	48% $^5\Pi$ + 35% $^5\Sigma^-$ + 14% $^5\Delta$
$^5\Pi_2$	2	1.416	43% $^5\Pi$ + 32% $^5\Delta$ + 16% $^5\Sigma^-$ + 7% $^5\Phi$
$^5\Phi_4$	4	1.438	50% $^5\Phi$ + 40% $^5\Delta$ + 9% $^5\Gamma$
$^5\Delta_3$	3	1.444	50% $^5\Delta$ + 22% + 21% $^5\Phi$
$^3\Gamma_5$	5	1.473	47% $^3\Gamma$ + 17% $^5\Phi$ + 15% $^3\Gamma$ + 10% ^3H + 6% $^5\Gamma$ + 5% ^5H
$^3H_6$	6	1.477	98% ^3H + 2% ^3H
$^3\Phi_4$	4	1.532	47% $^3\Phi$ + 24% $^3\Gamma$ + 12% $^5\Gamma$ + 8% $^5\Delta$
$^3\Delta_3$	3	1.561	37% $^3\Delta$ + 33% $^3\Phi$ + 13% ^5H + 5% $^3\Gamma$ + 5% $^5\Pi$
$^3\Delta_2$	2	1.565	40% $^3\Delta$ + 28% $^3\Pi$ + 9% $^3\Phi$ + 9% $^5\Phi$ + 8% $^5\Delta$ + 4% $^5\Sigma^-$
$^3\Pi_1$	1	1.573	43% $^3\Pi$ + 20% $^3\Sigma^-$ + 17% $^3\Delta$ + 9% $^5\Delta$ + 4% ^3H

https://doi.org/10.1021/acs.jpca.2c06978
J. Phys. Chem. A 2022, 126, 9392−9407

Table 3. continued

state	Ω	ΔE (eV)	ΛS composition
$^3\Pi_0$	0	1.577	41% $^3\Pi$ + 39% $^3\Sigma^-$ + 12% $^5\Pi$ + 6% $^5\Delta$
$^3\Gamma_5$	5	1.637	67% $^3\Gamma$ + 22% $^3\Gamma$ + 10% ^{3}H

Table 4. SO-CASPT2/aQ-PP Spectroscopic Parameters for Selected Low-Lying Ω States of UC

Ω state	T_e (cm^{-1})	r_e (Å)	ω_e (cm^{-1})	$\omega_e x_e$ (cm^{-1})	B_e (cm^{-1})
$^5H_3$	0	1.854	949.6	0.1	0.429
$^5H_4$	403	1.855	952.9	2.7	0.429
$^5\Gamma_2$	1557	1.860	965.6	9.6	0.426
$^5\Pi_1$	1903	1.855	890.2	5.3	0.429
$^5\Phi_3$	1920	1.863	950.4	11.5	0.425
$^5\Pi_0$	2000	1.854	953.3	7.1	0.429
$^5\Pi_2$	2178	1.864	924.2	3.0	0.425
$^3H_4$	2186	1.857	967.8	6.8	0.428
$^5H_5$	2242	1.869	1007.4	3.6	0.422
$^5\Phi_1$	2815	1.858	962.2	2.6	0.428
$^5\Delta_0$	2887	1.858	951.9	10.1	0.427
$^5\Phi_4$	3702	1.860	916.5	5.8	0.426
$^5\Gamma_3$	3750	1.860	988.0	5.3	0.427
$^5\Sigma_2^-$	4323	1.854	951.7	6.4	0.429
$^5\Pi_1$	4517	1.856	1011.7	10.0	0.428
$^5\Delta_0$	4670	1.859	970.4	6.2	0.427
$^3\Gamma_3$	5114	1.865	853.7	8.4	0.424
$^5H_6$	5154	1.858	965.5	4.7	0.428
$^3\Delta_1$	5751	1.854	923.5	14.9	0.429
$^3H_4$	5823	1.855	967.2	14.6	0.429
$^5H_5$	6170	1.866	872.3	10.0	0.424
$^3\Pi_0$	6291	1.860	920.9	3.2	0.427
$^5\Gamma_4$	6469	1.863	919.2	3.9	0.425
$^3\Phi_2$	6694	1.856	903.0	1.2	0.428
$^5\Phi_3$	6711	1.857	934.7	4.5	0.428
$^3H_5$	6952	1.857	946.1	9.3	0.428
$^3\Delta_2$	7001	1.858	947.1	6.7	0.428
$^5\Delta_1$	7009	1.856	964.1	4.3	0.429
$^5\Delta_0$	7041	1.855	990.0	9.5	0.429
$^3\Gamma_3$	7590	1.866	811.4	9.7	0.424
$^3\Delta_1$	7807	1.857	982.3	14.3	0.428

corresponding to these peaks are difficult without a higher resolution spectrum.

Using the ground state of UC^-, eight states are predicted to fall between ~1.70 and 1.90 eV, where there is still intensity in the spectrum in the high valley before the peak at ~2.0 eV. The next assigned EBE at 1.990 eV has three states as potential candidates, all of them quintets. There are four states ($^5\Pi_1$, $^5\Delta_0$, $^3\Gamma_3$, $^5H_6$) that are consistent with the EBE of 2.112 eV. The experimental peak at 2.316 eV could be attributed to two states, one triplet and one quintet. Our calculations predicted eight states between ~2.34 and ~2.5 eV. Lower-intensity peaks, compared to the previous, in the region of 2.5 and 3.0 eV can be accounted for by 27 states. An additional state is predicted at ~3.15 eV.

To account for transitions below the first VDE, there are two possibilities. It is possible that there are transitions from excited vibrational states of the ground state of the anion. These vibrational states are at 0.12, 0.24, and 0.35 eV above the ground state leading to first VDE values of 1.38, 1.26, and 1.15 eV, which can readily account for the observed shoulder at 1.1−1.3 eV as well as the width of the VDE peak. In addition, the first excited state of UC^- ($^4\Gamma_{7/2}$) is only 0.079 eV (637 cm^{-1}) higher than the ground state so it can also contribute to the lower energies in the PES spectrum with a VDE value of 1.42 eV. The vibrational states, v = 1, 2, and 3, of the first electronic excited state of UC^- may also be populated. These vibrational states have respective VDEs of 1.30, 1.19, and 1.07 eV and could contribute to the intensity of the shoulder at low energy. If we consider detachment from the second excited electronic state of UC^- ($^2\Phi_{5/2}$), located 0.164 eV (1323 cm^{-1}) higher than the ground state, a VDE of 1.34 eV is predicted with corresponding VDEs of 1.22 and 1.11 eV from the vibrationally excited v = 1 and 2 states of this second electronically excited state, respectively. Clearly, if these electronic and vibrational states are populated as seems likely based on the observed shoulder to lower energy from the VDE, they could also contribute to the higher energy transitions in the PES spectra further complicating the assignments.

Calculated Properties of UC^+. The ionization energy (IE) of UC (UC ($^5H_3$) → UC^+ ($^4H_{7/2}$) + e$^-$) at the FPD level is predicted to be 6.343 eV (612.0 kJ/mol) (Table 5). This value is very similar to the IE of UN (6.301 eV) and slightly higher than the IE of the uranium atom (6.1939 eV).[59] As found for the AEA, the additional FPD components beyond CCSD(T) make small contributions to the CBS value, with the ΔE_{CV} being the largest one. In this case, the difference between IE(CBS) and the final FPD value is 0.009 eV.

The potential energy curves calculated for the doublet and quartet low-lying states of UC^+ are shown in Figure 4 and the assigned states are shown in Table 7 with the spectroscopic constants in Table 8. The ground state is predicted at the SO-CASPT2 level to be $^4H_{7/2}$. The first excited state ($^4H_{9/2}$) lies higher in energy by 0.130 eV (1049 cm^{-1}). Note that for the three molecules $UC^{0/+/-}$, the two lowest-lying states arise from the spin−orbit splitting of the same ΛS state. Although the ground states of UC, UC^- and UC^+ are almost a pure spin state (see Tables 1, 3, and 7), the first excited state of each is a mixture of states including those with different multiplicities. This suggests a contribution from second-order spin−orbit effects and strong coupling of off-diagonal terms in the spin−orbit matrix which shifts this state to lower energies in all three. The CCSD(T) calculation predicts r_e = 1.837 Å and ω_e = 965.7 cm^{-1} which are consistent with the SO-CASPT2 values of r_e = 1.825 Å and ω_e = 963.8 cm^{-1}. The value of r_e for UC^+ is 0.029 Å shorter than r_e(UC) and the corresponding ω_e for UC^+ is 14 cm^{-1} higher than for UC. The spin−orbit correction for UC^+ is 0.633 eV (5102 cm^{-1}). Note that the ground states of all of the $UC^{0/+/-}$ molecules have similar SO corrections of ~5100 cm^{-1}. The electronic configuration of the ground state of UC^+ resembles that of UC^- with three unpaired electrons, two in the 5f orbitals (fφ, fδ), and a singly occupied U-C σ bond. The difference is in the 7s orbital on the U where UC^- has two additional electrons in the 7s and in the 5f orbitals that are occupied, fφ and fδ in UC^+, and, fφ and fπ in UC^-. The only change in the UC ground-state configuration compared to UC^+ is that it has a single unpaired 7s electron.

https://doi.org/10.1021/acs.jpca.2c06978
J. Phys. Chem. A 2022, 126, 9392−9407

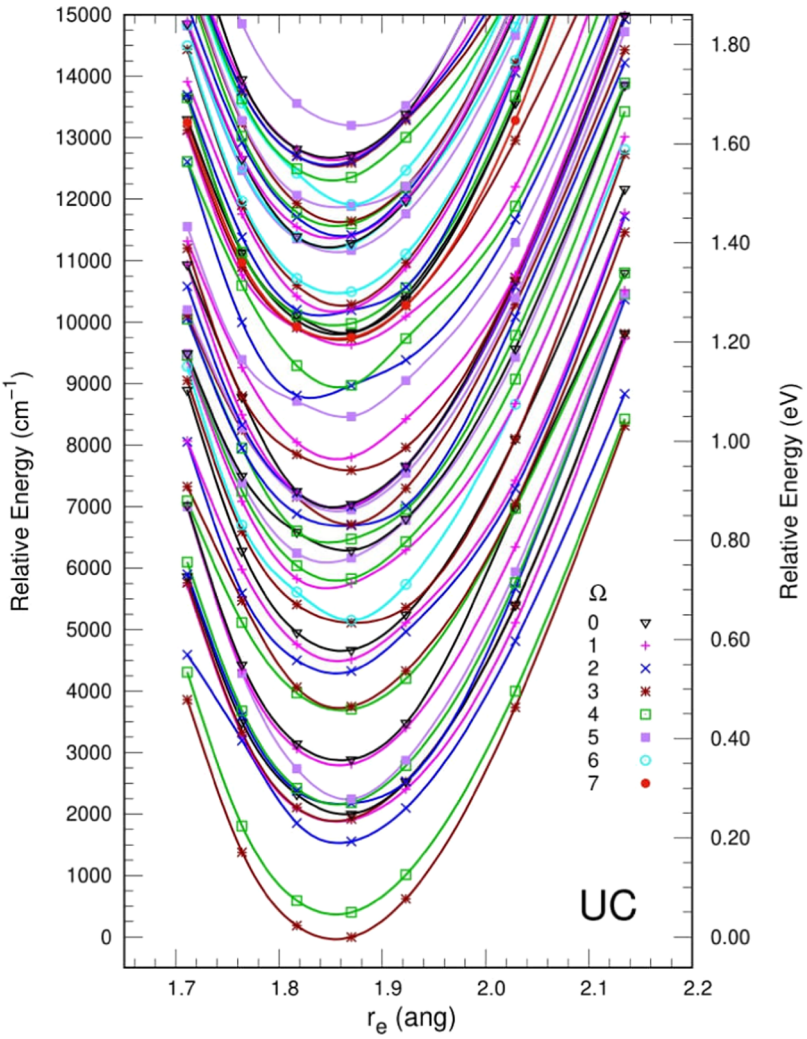

Figure 3. SO-CASPT2/aQ-PP potential energy curves for the low-lying Ω states of UC.

Table 5. FPD Components for EA and Ionization Energy (IE) of UC at 0 K with DK Basis Sets in eV

property	AEA	VDE[h]	IE
awD-DK	1.316	1.325	6.310
awT-DK	1.332	1.336	6.318
awQ-DK	1.440	1.447	6.328
ΔE_{CBS}[a]	1.511	1.521	6.334
ΔE_{CV}[b]	0.020		0.047
ΔE_{ZPE}[b]	0.003		−0.004
ΔE_{SO}[c]	−0.016		−0.006
ΔE_{Gaunt}[d]	0.005		0.008
ΔE_{QED}[e]	−0.010		−0.017
ΔE_T[f]	−0.012		−0.015
ΔE_Q[g]	−0.008		−0.004
total	1.493	1.500[i]	6.343

[a]CCSD(T) value extrapolated to the CBS limit using aw*n*-DK basis sets for *n* = D, T, Q. [b]CCSD(T)/awQ-DK. [c]SO-CASPT2 values: UC = 0.639 eV (5151 cm^{-1}), UC$^-$ = 0.622 eV (5019 cm^{-1}), UC$^+$ = 0.633 eV (5102 cm^{-1}). [d]Fully uncontracted cc-pVDZ-DK3. [e]Correction for the Lamb shift. [f]ΔE_T = CCSDT − CCSD(T). [g]ΔE_Q = CCSDT(Q) − CCSDT. [h]UC ($^5H_3$) at UC$^-$ ($^4\Gamma_{5/2}$) geometry for each level of theory. The CCSD(T)/CBS value is added to the AEA. [i]Value does not include a ZPE correction but includes the same other corrections as calculated for the AEA.

Thermochemistry. The dissociation energies of the UC and UC$^+$ species were calculated at the FPD level. The results are summarized in Table 9. The UC dissociation energy is calculated relative to the U$^+$ + C asymptote due to the difficulty in calculating the energy of U with CCSD(T) and then corrected to the U + C asymptote using the experimental IE(U).[59] The BDE for UC$^+$ is for the channel U$^+$ + C as IE(U) is less than that of IE(C). The BDE(UC$^-$) is obtained from the electron affinity of UC and is for the channel U + C$^-$ as the electron affinity of C is 1.262114 ± 0.000044[60] and that for U is 0.309 ± 0.025 eV.[17] The BDEs of UC, UC$^+$, and UC$^-$ are calculated to be 411.3 kJ/mol (4.26 eV), 396.0 kJ/mol (4.10 eV), and 433.6 kJ/mol (4.49 eV), respectively. A direct calculation of the UC bond energy with respect to the U + C asymptote gives a value of 419.0 kJ/mol, which differs from the value given above by ∼8 kJ/mol, most likely due to the difficulty of calculating the energy of U at the CCSD(T) level. Our results for BDE(UC) at the FPD level are higher by about 0.1 eV compared to the calculated value of 402 kJ/mol obtained by Pogány et al.[14] at the SO-CASPT2 level. Note that the SO-CASPT2 calculations in the current work give a lower value of 390.0 kJ/mol (4.04 eV).

The SO correction to the BDE of −18.9 kJ/mol for UC includes −61.6 kJ/mol (−5151 cm^{-1}) for UC, −80.2 kJ/mol (−6704 cm^{-1}) for U$^+$ and −0.35 kJ/mol (29.6 cm^{-1}) for C.

https://doi.org/10.1021/acs.jpca.2c06978
J. Phys. Chem. A 2022, 126, 9392−9407

Table 6. Calculated VDEs at the SO-CASPT2/aQ-PP Level of Theory

state	VDE (eV)	state	VDE (eV)	state	VDE (eV)
$^5H_3$	1.500	$^5H_5$	2.265	$^3\Pi_2$	2.764
$^5H_4$	1.550	$^3\Pi_0$	2.280	$^3\Sigma_1^-$	2.767
$^5\Gamma_2$	1.693	$^5\Gamma_4$	2.302	$^3\Delta_3$	2.775
$^5\Pi_1$	1.736	$^3\Phi_2$	2.330	$^5\Gamma_6$	2.801
$^5\Phi_3$	1.738	$^5\Phi_3$	2.332	$^5\Phi_5$	2.884
$^5\Pi_0$	1.748	$^3H_5$	2.362	$^3H_6$	2.896
$^5\Pi_2$	1.770	$^3\Delta_2$	2.368	$^5\Pi_0$	2.900
$^3H_4$	1.771	$^5\Delta_1$	2.369	$^5\Pi_1$	2.915
$^5H_5$	1.778	$^5\Delta_0$	2.373	$^5\Pi_2$	2.916
$^5\Phi_1$	1.849	$^3\Gamma_3$	2.441	$^5\Phi_4$	2.938
$^5\Delta_0$	1.858	$^3\Delta_1$	2.468	$^5\Delta_3$	2.944
$^5\Phi_4$	1.959	$^3H_5$	2.550	$^3\Gamma_5$	2.973
$^5\Gamma_3$	1.965	$^3\Delta_2$	2.612	$^3H_6$	2.977
$^5\Sigma_2^-$	2.036	$^3\Gamma_4$	2.612	$^3\Phi_4$	3.032
$^5\Pi_1$	2.060	$^3\Sigma_1^-$	2.694	$^3\Delta_3$	3.061
$^5\Delta_0$	2.079	$^3\Delta_3$	2.706	$^3\Delta_2$	3.065
$^3\Gamma_3$	2.134	$^5H_7$	2.709	$^3\Pi_1$	3.073
$^5H_6$	2.139	$^3\Sigma_0^-$	2.718	$^3\Pi_0$	3.077
$^3\Delta_1$	2.213	$^3\Pi_0$	2.719	$^3\Gamma_5$	3.137
$^3H_4$	2.222	$^3\Gamma_4$	2.737		

The SO correction of −19.5 kJ/mol for UC^+ includes −61.03 kJ/mol (−5102 cm^{-1}) and the above values for U^+ and C. The atomic corrections are consistent with the values obtained from the expression $\Sigma_J(2J + 1)E(J)/\Sigma_J(2J + 1)$ using the ground state values for $E(J)$ which gives 29.6 cm^{-1} for C and 6851 cm^{-1} for U^+.[61] Compared to UN and UN^+, the BDE(UC) is considerably lower, by around 150 kJ/mol. Using the experimental BDE of ThC (5.060(3) eV) reported by Sevy et al.,[62] the UC bond is ∼15% weaker than the ThC bond.

The heats of formation of UC and UC^+ were obtained from the expression $\Delta H_f^\circ(0\ K)\ UC^{0/+} = \Delta H_f^\circ(0\ K)\ U^{0/+} + \Delta H_f^\circ(0\ K)\ C - BDE(UC^{0/+})$. These results are shown in Table 10. We used the known experimental atomic energies of $\Delta H_f^\circ(0\ K)$ of U (ΔH_f° (0 K) = 533.0 ± 8 kJ/mol), and C (ΔH_f° (0 K) = 711.4 kJ/mol) from the active thermochemical tables (ATcT).[63−65] The ΔH_f° (0 K) (UC^-) was computed to be 689.0 kJ/mol using the AEA and ΔH_f° (0 K) of UC. We calculated heats of formation at 298 K using the approach for the thermal corrections described by Curtiss et al.[66] and the 6.36 and 0.25 kJ/mol thermal corrections of U and C, respectively.[67]

Electronic Structure Analysis. Natural bond orbital calculations were carried out for the $UC^{\circ/+/-}$ molecules. The natural population analysis (NPA) charges (q) and populations for the 5f, 6d, and 7s orbitals of U and 2s and 2p orbitals of C are shown in Table 11. The NBO analysis (Table 12) reveals that each of the UC molecules studied contains significant covalent interactions. As noted above, the ground state for UC has three unpaired electrons on the U (5fφ, 5fδ,

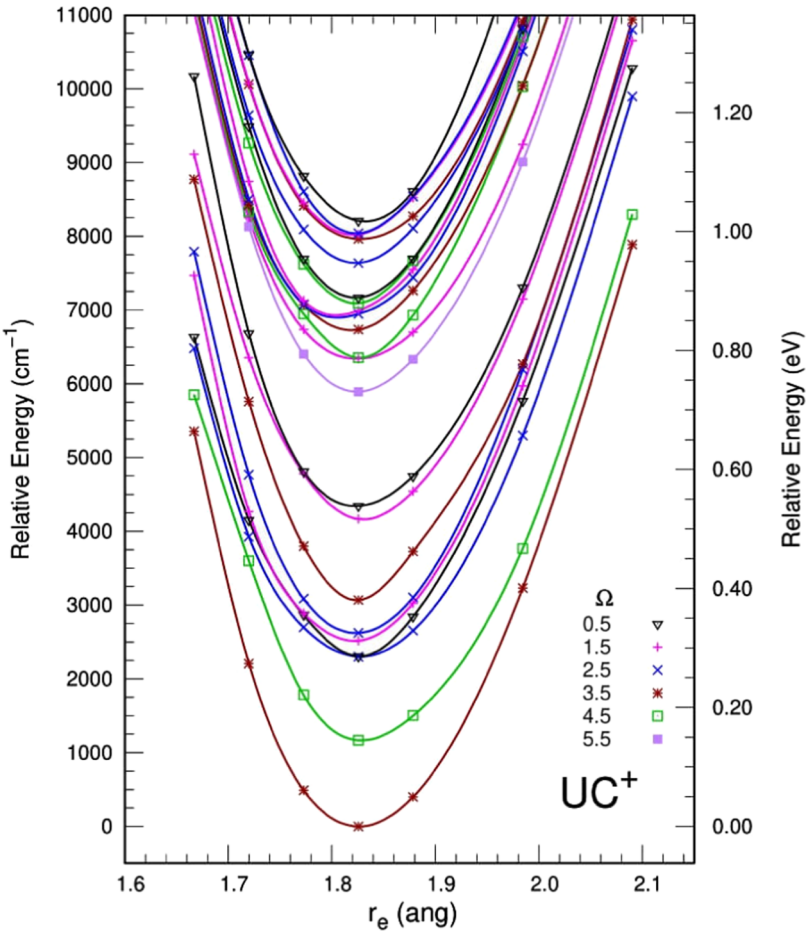

Figure 4. SO-CASPT2/aQ-PP potential energy curves for the low-lying Ω states of UC^+.

https://doi.org/10.1021/acs.jpca.2c06978
J. Phys. Chem. A 2022, 126, 9392−9407

Table 7. Low-Lying States of UC^+ at the CASPT2/aQ-PP + SO Level

state	Ω	ΔE (eV)	ΛS composition
$^4H_{7/2}$	3.5	0.000	82% ^4H + 9% $^4\Gamma$ + 8% $^2\Gamma$
$^4H_{9/2}$	4.5	0.130	42% ^4H + 33% ^2H + 10% $^4\Gamma$ + 9% $^2\Gamma$ + 4% $^2\Gamma$
$^4\Gamma_{5/2}$	2.5	0.275	67% $^4\Gamma$ + 23% $^4\Phi$ + 7% $^4\Delta$
$^4\Pi_{1/2}$	0.5	0.297	49% $^4\Pi$ + 38% $^4\Sigma^-$ + 12% $^4\Delta$
$^4\Pi_{3/2}$	1.5	0.313	34% $^4\Pi$ + 28% $^4\Delta$ + 17% $^4\Sigma^-$ + 10% $^4\Phi$ + 7% $^2\Delta$
$^2\Phi_{5/2}$	2.5	0.324	40% $^2\Phi$ + 18% $^2\Delta$ + 16% $^4\Delta$ + 13% $^4\Gamma$ + 9% $^4\Pi$
$^4\Gamma_{7/2}$	3.5	0.367	31% $^4\Gamma$ + 30% $^2\Gamma$ + 20% $^4\Phi$ + 10% $^2\Phi$ + 5% $^4\Delta$
$^4\Phi_{3/2}$	1.5	0.491	51% $^4\Phi$ + 15% $^2\Delta$ + 12% $^2\Pi$ +11% $^4\Sigma^-$ + 9% $^4\Delta$
$^4\Delta_{1/2}$	0.5	0.512	37% $^4\Delta$ + 34% $^4\Pi$ + 12% $^2\Sigma^-$ + 11% $^2\Pi$ + 5% $^4\Sigma^-$
$^4H_{11/2}$	5.5	0.731	72% ^4H + 15% ^2H + 13% $^4\Gamma$
$^4\Phi_{3/2}$	1.5	0.782	90% $^4\Phi$ + 7% $^4\Delta$
$^4H_{9/2}$	4.5	0.783	53% ^4H + 29% ^2H + 13% $^2\Gamma$
$^4\Gamma_{7/2}$	3.5	0.817	43% $^4\Gamma$ + 31% $^2\Phi$ + 11% $^4\Delta$ + 7% ^4H + 4% $^2\Gamma$
$^2\Phi_{5/2}$	2.5	0.841	38% $^2\Phi$ + 38% $^4\Pi$ + 20% $^4\Delta$
$^4\Sigma^-_{3/2}$	1.5	0.857	46% $^4\Sigma^-$ + 33% $^2\Delta$ + 14% $^4\Delta$
$^4\Gamma_{9/2}$	4.5	0.863	53% $^4\Gamma$ + 21% ^2H + 20% $^4\Phi$ + 5% $^2\Gamma$
$^4\Pi_{1/2}$	0.5	0.896	52% $^4\Pi$ + 26% $^4\Delta$ + 11% $^2\Pi$ + 7% $^4\Sigma^-$
$^4\Phi_{5/2}$	2.5	0.908	44% $^4\Phi$ + 26% $^2\Delta$ + 13% $^4\Gamma$ + 12% $^4\Pi$ + 4% $^4\Delta$
$^2\Gamma_{7/2}$	3.5	0.964	42% $^2\Gamma$ + 28% $^4\Delta$ + 24% $^4\Phi$
$^4\Phi_{3/2}$	1.5	0.970	30% $^4\Phi$ + 29% $^2\Pi$ + 16% $^4\Pi$ + 13% $^2\Delta$ + 10% $^4\Delta$
$^4\Phi_{5/2}$	2.5	0.992	86% $^4\Phi$ + 12% $^4\Delta$
$^2\Sigma^-_{1/2}$	0.5	1.004	39% $^2\Sigma^-$ + 33% $^2\Pi$ + 13% $^4\Delta$ + 8% $^4\Sigma^-$ + 5% $^4\Pi$
$^4\Phi_{7/2}$	3.5	1.097	62% $^4\Phi$ + 25% $^2\Gamma$ + 6% $^4\Delta$ + 3% ^4H
$^2\Gamma_{9/2}$	4.5	1.114	41% $^2\Gamma$ + 40% $^4\Phi$ + 11% ^2H + 6% $^4\Phi$
$^4\Delta_{1/2}$	0.5	1.183	96% $^4\Delta$
$^4H_{13/2}$	6.5	1.301	100% ^4H
$^4\Sigma^-_{1/2}$	0.5	1.327	71% $^4\Sigma^-$ + 13% $^4\Sigma^-$ + 12% $^4\Pi$
$^4\Sigma^-_{3/2}$	1.5	1.330	65% $^4\Sigma^-$ + 11% $^4\Delta$ + 8% $^4\Pi$ + 7% $^4\Sigma^-$ + 4% $^4\Delta$
$^4\Delta_{3/2}$	1.5	1.371	70% $^4\Delta$ + 21% $^4\Sigma^-$ + 6% $^4\Phi$
$^4\Gamma_{11/2}$	5.5	1.398	78% $^4\Gamma$ + 20% ^4H
$^4\Pi_{5/2}$	2.5	1.435	34% $^4\Pi$ + 25% $^4\Delta$ + 18% $^2\Delta$ + 13% $^4\Delta$ + 7% $^2\Phi$
$^4\Pi_{1/2}$	0.5	1.444	38% $^4\Pi$ + 28% $^4\Sigma^-$ + 28% $^4\Sigma^-$ + 6% $^4\Delta$
$^4\Pi_{3/2}$	1.5	1.466	36% $^4\Pi$ + 19% $^4\Delta$ + 15% $^4\Sigma^-$ + 11% $^4\Sigma^-$ + 10% $^4\Delta$
$^2\Gamma_{7/2}$	3.5	1.483	29% $^2\Gamma$ + 25% $^2\Phi$ + 14% $^4\Phi$ + 11% $^4\Phi$ + 8% $^4\Delta$ + 5% $^4\Gamma$
$^4\Delta_{7/2}$	3.5	1.493	44% $^4\Delta$ + 19% $^2\Phi$ + 14% $^4\Delta$ + 12% $^4\Phi$ + 11% $^2\Gamma$
$^4\Phi_{9/2}$	4.5	1.520	53% $^4\Phi$ + 34% $^4\Gamma$ + 7% $^2\Gamma$
$^2\Delta_{5/2}$	2.5	1.548	35% $^2\Delta$ + 22% $^4\Delta$ + 14% $^2\Phi$ + 13% $^4\Phi$ + 10% $^4\Delta$
$^2H_{11/2}$	5.5	1.549	83% ^2H + 9% $^4\Gamma$ + 8% ^4H
$^4\Delta_{5/2}$	2.5	1.578	52% $^4\Delta$ + 18% $^4\Delta$ + 14% $^4\Phi$ + 7% $^4\Phi$ + 5% $^4\Pi$
$^4\Phi_{7/2}$	3.5	1.593	30% $^4\Phi$ + 23% $^2\Gamma$ + 14% $^4\Delta$ + 10% $^4\Gamma$ + 8% $^4\Delta$ + 7% $^2\Phi$
$^2\Pi_{3/2}$	1.5	1.632	51% $^2\Pi$ + 27% $^2\Delta$ + 13% $^4\Delta$ + 4% $^4\Phi$
$^2\Gamma_{9/2}$	4.5	1.665	70% $^2\Gamma$ + 16% $^4\Phi$ + 5% ^2H + 4% $^4\Phi$
$^2\Sigma^-_{1/2}$	0.5	1.675	43% $^2\Sigma^-$ + 43% $^2\Pi$ + 5% $^4\Pi$
$^4\Delta_{7/2}$	3.5	1.745	58% $^4\Delta$ + 20% $^4\Phi$ + 11% $^2\Gamma$ + 6% $^2\Phi$
$^4\Phi_{9/2}$	4.5	1.875	50% $^4\Phi$ + 46% $^2\Gamma$
$^4\Delta_{7/2}$	3.5	2.164	100% $^4\Delta$
$^4\Delta_{5/2}$	2.5	2.314	83% $^4\Delta$ + 17% $^4\Delta$
$^4\Sigma^-_{1/2}$	0.5	2.349	100% $^4\Sigma^-$
$^4\Sigma^-_{3/2}$	1.5	2.349	100% $^4\Sigma^-$
$^4\Delta_{3/2}$	1.5	2.463	100% $^4\Delta$
$^4\Delta_{1/2}$	0.5	2.613	100% $^4\Delta$

7s) and a singly occupied U-C σ bond. For UC^-, the U has a 5fπ, 5fφ configuration and there is a singly occupied U-C σ bond, whereas for UC^+, the U has a 5fφ, 5fδ, configuration and there is a singly occupied U-C σ bond. The UC ^5H molecular state has a $5f^27s^1$ configuration on the U corresponding to a U(III) in the ^4H state. This electronic configuration on the U is the same as that for UN but now there is a singly occupied U-C σ bond instead of a doubly occupied U-N σ bond.[15] The unpaired electron on the C couples with the quartet state on the U in UC to give a diatomic quintet state instead of the lone

https://doi.org/10.1021/acs.jpca.2c06978
J. Phys. Chem. A 2022, 126, 9392−9407

Table 8. SO-CASPT2/aQ-PP Spectroscopic Parameters for Selected Low-Lying Ω States of UC^+

Ω state	T_e (cm^{-1})	r_e (Å)	ω_e (cm^{-1})	$\omega_e x_e$ (cm^{-1})	B_e (cm^{-1})
$^4H_{7/2}$	0	1.825	963.8	5.7	0.443
$^4H_{9/2}$	1049	1.829	963.6	7.0	0.441
$^4\Gamma_{5/2}$	2218	1.829	912.0	7.0	0.441
$^4\Pi_{1/2}$	2395	1.840	918.0	2.9	0.436
$^4\Pi_{3/2}$	2525	1.821	964.9	2.9	0.445
$^2\Phi_{5/2}$	2613	1.823	1000.7	2.4	0.444
$^4\Gamma_{7/2}$	2960	1.836	995.5	2.8	0.438
$^4\Phi_{3/2}$	3960	1.837	938.9	1.4	0.437
$^4\Delta_{1/2}$	4130	1.824	909.6	10.7	0.443
$^4H_{11/2}$	5896	1.825	1000.1	4.7	0.443
$^4\Phi_{3/2}$	6307	1.821	957.5	13.3	0.445
$^4H_{9/2}$	6315	1.836	960.3	1.0	0.438
$^4\Gamma_{7/2}$	6590	1.819	968.5	6.9	0.446
$^2\Phi_{5/2}$	6783	1.813	992.0	3.5	0.449
$^4\Sigma_{3/2}^-$	6912	1.817	995.4	2.8	0.447
$^4\Gamma_{9/2}$	6961	1.826	1014.3	3.7	0.442
$^4\Pi_{1/2}$	7227	1.825	1045.6	5.8	0.443
$^4\Phi_{5/2}$	7324	1.825	955.7	2.1	0.443
$^2\Gamma_{7/2}$	7775	1.824	930.8	6.3	0.445
$^4\Phi_{3/2}$	7824	1.823	944.1	3.3	0.444
$^4\Phi_{5/2}$	8001	1.828	962.1	5.7	0.442
$^2\Sigma_{1/2}^-$	8098	1.824	1036.0	5.8	0.443

Table 9. FPD Components for the BDE of UC and UC^+ ($UC^+ \rightarrow U^+ + C$) in kJ/mol

component	UC[a]	UC^+
awd-DK	976.5	367.7
awt-DK	982.0	372.4
awq-DK	987.4	376.8
ΔE_{CBS}[b]	990.8	379.6
ΔE_{CV}	20.1	24.7
ΔE_{SO}	−18.9	−19.5
ΔE_{Gaunt}	5.3	0.9
ΔE_{QED}	0.3	1.2
ΔE_{CCSDT}	12.5	14.0
ΔE_{CCSDTQ}	4.3	1.1
ΔE_{ZPE}[c]	−5.5	−5.8
IE(U)[d]	−597.6	
D_0 (0 K)	411.3	396.0

[a]The dissociation of UC was calculated to the U^+ + C asymptote and then corrected with the experimental IE(U). [b]CCSD(T) value extrapolated to the CBS limit using aw*n*-DK basis sets for *n* = D, T, Q. [c]CCSD(T)/awQ-DK. [d]Experimental ionization energy of U.[59]

Table 10. Heats of Formation ($\Delta H_f°$) and BDEs (D_0) of $UC^{0/-/+}$ in kJ/mol

diatomic	$\Delta H_f°$(0 K)	$\Delta H_f°$(298 K)	D_0
UC	833.1	830.9	411.3
UC^-	689.0	686.8	433.6[a]
UC^+	1448.3	1446.1	396.0[b]

[a]To U + C^-. [b]To U^+ + C.

pair on N in UN that results in a quartet state. Thus, the oxidation state of U in UC is like that of U in UN. The UN, UN^-, and UN^+ ground states have predominantly ^{x}H ΛS state character. Whereas this same H ground state is predicted for

Table 11. Natural Population Analysis (NPA) from the Natural Bond Orbitals (NBOs) for the Charges (q) and Total Atomic Orbital Populations for $UC^{0/-/+}$ at the HF/aD-DK Level

property	UC ($^5H_3$)	UC^- ($^4\Gamma_{5/2}$)	UC^+ ($^4H_{7/2}$)
q(U)	0.761	0.039	1.600
q(C)	−0.761	−1.039	−0.600
5f (5fα/5fβ)	2.99 (2.57/0.42)	2.81 (2.40/0.41)	3.18 (2.73/0.44)
6d (6dα/6dβ)	1.36 (0.85/0.51)	1.47 (0.92/0.56)	1.28 (0.75/0.53)
7s (7sα/7sβ)	0.98 (0.92/0.06)	1.85 (0.93/0.92)	0.06 (0.03/0.03)
C 2s (2sα/2sβ)	1.75 (0.91/0.84)	1.76 (0.91/0.85)	1.76 (0.91/0.85)
C 2p (2pα/2pβ)	2.97 (1.73/1.24)	3.10 (1.81/1.28)	2.82 (1.61/1.21)

UC and UC^+, UC^- has a $^4\Gamma$ ground state. Even though, comparing isoelectronic molecules to predict their ground state works in many cases, for the actinide diatomics in the current study, this concept only applies to the actinide metal configuration. Thus, UN^+ will be isoelectronic with UC^+ as shown by the comparable H ground states, but this does not hold for comparing UN^- and UC^-, although the metal has the same configuration.

The concept of isoelectronic metal structure cannot be extended from UC with a $5f^27s^1$ U configuration and a ^{4}H atomic U state and UN with a $5f^27s^1$ U configuration and ^{4}H atomic U state to UO and UF. For UO, the metal oxidation state changes to give UO with a $5f^37s^1$ U configuration and a ^{5}I atomic U state[68,69] with the addition of a 5f electron. The U oxidation state further changes in going to UF, where the U electrons are configured as $5f^37s^2$ with a ^{4}I atomic U state,[70−72] having added a 7s electron to the configuration found for UO. In comparing the U configuration in UF to the ground configuration in the uranium atom, it is clear that the oxidation to U^+ has resulted in the loss of the 6d electron. Thus, UO has the same electronic configuration on U as found for UF^+ with the same ground state. Note that the UF configuration is essentially the same as that of UH ($5f^37s^2$ U configuration and a ^{4}I atomic U state).[73] In none of these molecules does the uranium configuration in the ground state contain an unpaired 6d electron. Our NBO calculations[15] on $UN^{0/+/-}$ predicted one electron (spin paired) in the 6d orbital due to backbonding from N to U and some d contribution to the bonding orbital.

The NPA charges (Table 11) predicted a $U^{0.8}C^{-0.8}$ charge distribution between the two atoms for UC which shows substantial ionic character. For UC^-, the negative charge on C changes somewhat from that in UC so that there is ca. −1 charge on the C and the additional electron goes mostly onto the U which now has a charge of ∼0. When an electron is removed from UC, it is removed from the uranium giving a $U^{+1.6}C^{-0.6}$ charge distribution. Again, the charge on the C undergoes only a small change.

The NPA (Table 11) shows that there is about one electron backbonding in the 5f and one electron backbonding in the 6d for UC. There are about 0.35 unpaired electrons in the 6d. There is one spin in the 7s on U. There are three electrons in the C 2p orbitals with 0.49 unpaired electrons in the 2p and a 0.07 unpaired spin in the C 2s. The electron added to UC to form UC^- predominantly goes into the 7s on U leading to a $7s^2$ occupancy. Only small changes are predicted for the remaining U and C orbitals. Removal of an electron from UC

https://doi.org/10.1021/acs.jpca.2c06978
J. Phys. Chem. A 2022, 126, 9392−9407

Table 12. Natural Bond Orbitals (NBOs) for $UC^{0/-/+}$ at the HF/aD-DK Level

			U					C		
molecule	NBO	occ	%q	%s	%p	%d	%f	%q	%s	%p
UC ($^5H_3$)	$\sigma_{U\text{-}C}$ α	1.000	50.3	6.7	7.5	31.1	54.6	49.7	13.7	86.0
	$\pi_{U\text{-}C}$ α	1.000	40.0	0.0	0.8	55.4	43.7	60.3	0.0	99.9
	$\pi_{U\text{-}C}$ β	1.000	40.1	0.0	0.8	50.3	48.9	59.9	0.0	99.9
	$\pi_{U\text{-}C}$ α	1.000	40.1	0.0	0.8	49.8	49.3	59.9	0.0	99.9
	$\pi_{U\text{-}C}$ β	1.000	40.1	0.0	0.8	49.8	49.3	59.9	0.0	99.9
UC^- ($^4\Gamma_{5/2}$)	$\sigma_{U\text{-}C}$ α	1.000	48.6	5.8	7.5	36.3	50.5	51.4	17.2	82.6
	$\pi_{U\text{-}C}$ α	1.000	34.8	0.0	0.8	81.6	17.6	65.2	0.0	99.9
	$\pi_{U\text{-}C}$ β	1.000	36.3	0.0	0.8	59.5	39.7	63.7	0.0	99.9
	$\pi_{U\text{-}C}$ α	1.000	39.7	0.0	0.8	46.3	52.9	60.3	0.0	99.9
	$\pi_{U\text{-}C}$ β	1.000	39.7	0.0	0.8	46.3	52.9	60.3	0.0	99.9
UC^+ ($^4H_{7/2}$)	$\sigma_{U\text{-}C}$ α	1.000	53.2	0.7	7.1	5.1	87.0	46.8	2.3	97.3
	$\pi_{U\text{-}C}$ α	1.000	42.2	0.0	1.0	47.4	51.6	57.8	0.0	99.9
	$\pi_{U\text{-}C}$ β	1.000	42.2	0.0	1.0	47.4	51.6	57.8	0.0	99.9
	$\pi_{U\text{-}C}$ α	1.000	40.7	0.0	0.9	54.7	44.3	59.3	0.0	99.9
	$\pi_{U\text{-}C}$ β	1.000	40.9	0.0	0.9	52.3	46.8	59.1	0.0	99.9

is from the U 7s orbital with again only small changes in the remaining orbitals. The basic electron configuration of UC ($7s^1$), UC^- ($7s^2$) and UC^+ ($7s^0$) molecules varies in terms of the occupation of the 7s orbital as found for UN, UN^+, and UN^-.[15,16] This shows that the C ligand is not affected by electron attachment or detachment processes as the 7s is a nonbonding orbital.

The bonding orbitals (Table 12) suggest a bond order of 2.5 for the UC bond with two doubly occupied U-C π bonds and a singly occupied U-C σ bond. There is a polarized $2s^2$ orbital on the C that delocalizes onto the U. The U-C π bonds have populations evenly split between the U and the C with mostly 6d and 5f characters on U and 2p character on the C. Similar results for the description of the bonding were reported by Wang et al.[12,13] and Pogány et al.[14] with effective bond orders between 2.0 and 3.0. The calculated bond distances for $UC^{0/+/-}$ are in the range of 1.8−1.9 Å falling between the value computed using the triple bond radii of C and U by Pyykkö[74] of 1.78 Å and the value of 2.01 Å computed with the double bond radii as would be expected for a molecule with a bond order of 2.5.

The two singly occupied 5f lone pairs on U for UC and UC^+ with one and zero electrons in the 7s orbital on U, respectively, are in the 5fφ and 5fδ orbitals where the two singly occupied 5f orbitals will minimize their interaction with the two U-C π bonding orbitals. When an additional electron is added to the 7s in UC to give the $7s^2$ configuration in UC^-, the energy of the 5fδ orbital is significantly raised so that the two singly occupied 5f electrons on the U are now in the 5fφ and 5fπ orbitals. Apparently, the repulsion between the $7s^2$ orbital and the 5fδ is larger than the interaction of the 5fπ with the U-C π bonds.

CONCLUSIONS

A detailed characterization of the UC, UC^-, and UC^+ molecules has been made using high-level electronic structure methods in combination with experimental PES spectra of UC^-. The ground and low-lying excited states of these species were elucidated and the spectroscopic constants were calculated. Due to the presence of occupied 5f electrons in U, the inclusion of SO effects resulted in a dense manifold of states with very small energetic separations. For UC, 59 states were found within ∼1.65 eV. A $^5H_3$ ground state is predicted for UC with an excited $^5H_4$ state only 0.050 eV higher in energy. The UC ground state configuration has unpaired electrons in the $5f^2$ and $7s^1$ orbitals on U and in a U-C σ bond with approximately equal contributions from the $2p_z$ on C and a mix of 5f and 6d on the U. Addition of an electron to UC to give UC^- ($^4\Gamma_{5/2}$) generates the $5f^27s^2$ configuration on U and removal of an electron to give UC^+ ($^4H_{7/2}$) generates the $5f^2$ configuration on U. The bond order of the U-C bonds remains at 2.5 for the three oxidation states. Compared to the isoelectronic molecules UN ($^4H_{7/2}$) and UN^+ ($^3H_4$), UC and UC^- show different ground states. In the case of UC, isoelectronic to UN^+, the quintet state is lower by 0.271 eV than the triplet $^3H_4$ state.

The adiabatic electron affinity (AEA) of UC is 1.493 eV at the FPD level and the ionization energy (IE) is 6.343 eV, both containing only small contributions from SO effects, −0.016 and −0.006 eV, respectively. The vertical detachment energies (VDE) for UC^- were calculated to better interpret the PES spectrum and are consistent with the assigned EBEs. The lowest VDE is predicted to be 1.500 eV. Considering electron detachments from the first excited state of UC^- ($^4\Gamma_{7/2}$), which is higher by only 0.079 eV (637 cm^{-1}), a VDE of 1.421 eV is obtained. The IE(UC) is very close energetically to the IE(UN) of 6.301 eV and slightly higher than the IE(U) of 6.1939 eV, suggesting that the ligand makes only a small contribution to this property.

The BDE of UC is estimated to be 411.3 kJ/mol, ∼15% weaker than the experimental BDE(ThC), and is significantly lower than those of UN (560.5 kJ/mol) and UN^+ (550.2 kJ/mol). The BDE of UC^- and UC^+ bracket BDE(UC). As predicted for the $UN^{0/-/+}$ diatomics, the anion (UC^-) has a BDE higher than the neutral and cation. The electronic structure analysis is consistent with a triple U≡C bond which varies between 1.8 and 1.9 Å for the UC molecules.

The NBOs show that the bonding on U is dominated by the 5f and 6d orbitals. A comparison of the behavior of UN and UC in three different oxidation states shows that the redox is all occurring in the 7s as the electronic structure of the U in both sets of molecules is the same, and there is effectively a triple bond to the ligand. Thus, C and N are behaving in a similar manner with the U-C having a bond order of 2.5 and U-N having a bond order of 3. For UO, only a double bond can be formed between U and O, and an additional electron is

https://doi.org/10.1021/acs.jpca.2c06978
J. Phys. Chem. A 2022, 126, 9392−9407

added to the U compared to UC and UN. This additional electron goes into the 5f to give a $5f^3 7s^1$ electron configuration on the U so that the U(II) is formed by loss of the 6d and a 7s electron. As only a single bond can be formed for UF, the U(I) has a $5f^3 7s^2$ electron configuration with loss of the 6d.

■ ASSOCIATED CONTENT

Supporting Information

The Supporting Information is available free of charge at https://pubs.acs.org/doi/10.1021/acs.jpca.2c06978.

Total energies at the CCSD(T) level, UCH adiabatic excitation energies; and complete citations for refs 28, 29, 48, 50, and 51 (PDF)

■ AUTHOR INFORMATION

Corresponding Authors

Kit H. Bowen − *Department of Chemistry, Johns Hopkins University, Baltimore, Maryland 21218, United States;* orcid.org/0000-0002-2858-6352; Email: kbowen@jhu.edu

David A. Dixon − *Department of Chemistry and Biochemistry, University of Alabama, Tuscaloosa, Alabama 35401, United States;* orcid.org/0000-0002-9492-0056; Email: dadixon@ua.edu

Authors

Gabriel F. de Melo − *Department of Chemistry and Biochemistry, University of Alabama, Tuscaloosa, Alabama 35401, United States*

Monica Vasiliu − *Department of Chemistry and Biochemistry, University of Alabama, Tuscaloosa, Alabama 35401, United States*

Gaoxiang Liu − *Department of Chemistry, Johns Hopkins University, Baltimore, Maryland 21218, United States;* orcid.org/0000-0002-1001-0064

Sandra Ciborowski − *Department of Chemistry, Johns Hopkins University, Baltimore, Maryland 21218, United States*

Zhaoguo Zhu − *Department of Chemistry, Johns Hopkins University, Baltimore, Maryland 21218, United States;* orcid.org/0000-0002-4395-9102

Moritz Blankenhorn − *Department of Chemistry, Johns Hopkins University, Baltimore, Maryland 21218, United States*

Rachel Harris − *Department of Chemistry, Johns Hopkins University, Baltimore, Maryland 21218, United States*

Chalynette Martinez-Martinez − *Department of Chemistry, Johns Hopkins University, Baltimore, Maryland 21218, United States*

Maria Dipalo − *Department of Chemistry, Johns Hopkins University, Baltimore, Maryland 21218, United States*

Kirk A. Peterson − *Department of Chemistry, Washington State University, Pullman, Washington 99164, United States;* orcid.org/0000-0003-4901-3235

Complete contact information is available at: https://pubs.acs.org/10.1021/acs.jpca.2c06978

Notes

The authors declare no competing financial interest.

■ ACKNOWLEDGMENTS

This work was supported by the U.S. Department of Energy (DOE), Office of Science, Office of Basic Energy Sciences, Heavy Element Chemistry program at Johns Hopkins University (K.H.B., experiment) through Grant Number, DE-SC0019317, at The University of Alabama (D.A.D., computational) through Grant No. DE-SC0018921, and at Washington State University (K.A.P., computational) through Grant No. DE-SC0008501. D.A.D. thanks the Robert Ramsay Fund at The University of Alabama.

■ REFERENCES

(1) Petti, D.; Crawford, D.; Chauvin, N. Fuels for Advanced Nuclear Energy Systems. *MRS Bull.* **2009**, *34*, 40−45.

(2) Vasudevamurthy, G.; Knight, T. Production of High Density Uranium Carbide Compacts for Use in Composite Nuclear Fuels. *Nucl. Technol.* **2008**, *163*, 321−327.

(3) Crawford, D. C.; Porter, D. L. Hayes. Fuels for Sodium-Cooled Fast Reactors: US Perspective. *J. Nucl. Mater.* **2007**, *371*, 202−231.

(4) Meyer, M. K.; Fielding, R.; Gan, J. Fuel Development for Gas-Cooled Fast Reactors. *J. Nucl. Mater.* **2007**, *371*, 281−287.

(5) Vasudevamurthy, G.; Nelson, A. T. Uranium Carbide Properties for Advanced Fuel Modeling—A Review. *J. Nucl. Mater.* **2022**, *558*, No. 153145.

(6) Freyss, M. First-Principles Study of Uranium Carbide: Accommodation of Point Defects and of Helium, Xenon, and Oxygen Impurities. *Phys. Rev. B* **2010**, *81*, No. 014101.

(7) Wdowik, U. D.; Piekarz, P.; Legut, D.; Jagło, G. Effect of Spin-orbit and On-site Coulomb Interactions on the Electronic Structure and Lattice Dynamics of Uranium Monocarbide. *Phys. Rev. B* **2016**, *94*, No. 054303.

(8) Petit, L.; Svane, A.; Szotek, Z.; Temmerman, W. M.; Stocks, G. M. Ground-State Electronic Structure of Actinide Monocarbides and Mononitrides. *Phys. Rev. B* **2009**, *80*, No. 045124.

(9) Ducher, R.; Duborg, R.; Barrachin, M.; Pasturel, A. First-principles Study of Defect Behavior in Irradiated Uranium Monocarbide. *Phys. Rev. B* **2011**, *83*, No. 104107.

(10) Yin, Q.; Kutepov, A.; Haule, K.; Kotliar, G.; Savrasov, S. Y.; Pickett, W. E. Electronic Correlation and Transport Properties of Nuclear Fuel Materials. *Phys. Rev. B* **2011**, *84*, No. 195111.

(11) Shi, H.; Zhang, P.; Li, S.-S.; Sun, B.; Wang, B. Electronic Structures and Mechanical Properties of Uranium Monocarbide from First-principles LDA + U and GGA + U Calculations. *Phys. Lett. A* **2009**, *373*, 3577−3581.

(12) Wang, X.; Andrews, L.; Malmqvist, P.-A.; Roos, B. O.; Gonçalves, A. P.; Pereira, C. C. L.; Marçalo, J.; Godart, C.; Villeroy, B. Infrared Spectra and Quantum Chemical Calculations of the Uranium Carbide Molecules UC and CUC with Triple Bonds. *J. Am. Chem. Soc.* **2010**, *132*, 8484−8488.

(13) Wang, X.; Andrews, L.; Ma, D.; Gagliardi, L.; Gonçalves, A. P.; Pereira, C. C. L.; Marçalo, J.; Godart, C.; Villeroy, B. Infrared Spectra and Quantum Chemical Calculations of the Uranium-Carbon Molecules UC, CUC, UCH, and $U(CC)_2$. *J. Chem. Phys.* **2011**, *134*, No. 244313.

(14) Pogány, P.; Kovács, A.; Visscher, L.; Konings, R. J. M. Theoretical Study of the Actinide Monocarbides (ThC, UC, PuC, and AmC). *J. Chem. Phys.* **2016**, *145*, No. 244310.

(15) de Melo, G. F.; Vasiliu, M.; Liu, G.; Ciborowski, S.; Zhu, Z.; Blankenhorn, M.; Harris, R.; Martinez-Martinez, C.; Dipalo, M.; Peterson, K. A.; Bowen, K. H.; Dixon, D. A. Electronic Properties of UN and UN^- from Photoelectron Spectroscopy and Correlated Molecular Orbital Theory. *J. Phys. Chem. A* **2022**, *126*, 7944−7953.

(16) Battey, S. R.; Bross, D. H.; Peterson, K. A.; Persinger, T. D.; VanGundy, R. A.; Heaven, M. C. Spectroscopic and Theoretical Studies of UN and UN^+. *J. Chem. Phys.* **2020**, *152*, No. 094302.

(17) Ciborowski, S. M.; Liu, G.; Blankenhorn, M.; Harris, R. M.; Marshall, M. A.; Zhu, Z.; Bowen, K. H.; Peterson, K. A. The Electron Affinity of the Uranium Atom. *J. Chem. Phys.* **2021**, *154*, No. 224307.
(18) Ho, J.; Ervin, K. M.; Lineberger, W. C. Photoelectron Spectroscopy of Metal Cluster Anions: Cu_n^-, Ag_n^-, and Au_n^-. *J. Chem. Phys.* **1990**, *93*, 6987−7002.
(19) Roos, B. O.; Taylor, P. R.; Siegbahn, P. E. M. A Complete Active Space SCF Method (CASSCF) Using a Density-matrix Formulated Super-CI Approach. *Chem. Phys.* **1980**, *48*, 157−173.
(20) Siegbahn, P. E. M.; Almlöf, J.; Heiberg, A.; Roos, B. O. The Complete Active Space SCF (CASSCF) Method in a Newton-Raphson Formulation with Application to the HNO Molecule. *J. Chem. Phys.* **1981**, *74*, 2384−2396.
(21) Andersson, K.; Malmqvist, P. A.; Roos, B. O.; Sadlej, A. J.; Wolinski, K. Second-Order Perturbation Theory with a CASSCF Reference Function. *J. Phys. Chem. A* **1990**, *94*, 5483−5488.
(22) Andersson, K.; Malmqvist, P. A.; Roos, B. O. Second-Order Perturbation Theory with a Complete Active Space Self-Consistent Field Reference Function. *J. Chem. Phys.* **1992**, *96*, 1218−1226.
(23) Dunning, T. H., Jr. Gaussian Basis Set for Use in Correlated Molecular Calculations. I. The Atoms Boron Through Neon and Hydrogen. *J. Chem. Phys.* **1989**, *90*, 1007−1023.
(24) Kendall, R. A.; Dunning, T. H., Jr; Harrison, R. J. Electron Affinities of the First-Row Atoms Revisited. Systematic Basis Sets and Wave Functions. *J. Chem. Phys.* **1992**, *96*, 6796−6806.
(25) Dolg, M.; Cao, X. Accurate Relativistic Small-core Pseudopotentials for Actinides. Energy Adjustment for Uranium and First Applications to Uranium Hydride. *J. Phys. Chem. A.* **2009**, *113*, 12573−12581.
(26) Peterson, K. A. Correlation Consistent Basis Sets for Actinides. I. The Th and U Atoms. *J. Chem. Phys.* **2015**, *142*, No. 074105.
(27) Ghigo, G.; Roos, B. O.; Malmqvist, P.-A. A Modified Definition of the Zeroth-Order Hamiltonian in Multiconfigurational Perturbation Theory (CASPT2). *Chem. Phys. Lett.* **2004**, *396*, 142−149.
(28) Werner, H.-J.; Knowles, P. J.; Manby, F. R.; Black, J. A.; Doll, K.; Heßelmann, A.; Kats, D.; Köhn, A.; Korona, T.; Kreplin, D. A.; et al. The Molpro Quantum Chemistry Package. *J. Chem. Phys.* **2020**, *152*, No. 144107.
(29) Werner, H.-J.; Knowles, P. J.; Knizia, G.; Manby, F. R.; Schütz, M.; Celani, P.; Györffy, W.; Kats, D.; Korona, T.; Lindh, R.; et al. *MOLPRO, version 2019.2, A Package of Ab Initio Programs*, 2021. https://www.molpro.net.
(30) Berning, A.; Schweizer, M.; Werner, H.-J.; Knowles, P. J.; Palmieri, P. Spin-orbit Matrix Elements for Internally Contracted Multireference Configuration Interaction Wavefunctions. *Mol. Phys.* **2000**, *98*, 1823−1833.
(31) Bross, D. H. Accurate *ab initio* Thermochemistry and Spectroscopy of Molecules Containing Transition Metals and Heavy Elements. Ph.D Thesis, Washington State University, 2015.
(32) Deegan, M. J. O.; Knowles, P. J. Perturbative Corrections to Account for Triple Excitations in Closed and Open Shell Coupled Cluster Theories. *Chem. Phys. Lett.* **1994**, *227*, 321−326.
(33) Rittby, M.; Bartlett, R. J. An Open-Shell Spin-Restricted Coupled Cluster Method: Application to Ionization Potentials in N_2. *J. Phys. Chem. A* **1988**, *92*, 3033−3036.
(34) Knowles, P. J.; Hampel, C.; Werner, H.-J. Coupled Cluster Theory for High Spin, Open Shell Reference Wave Functions. *J. Chem. Phys.* **1993**, *99*, 5219−5228.
(35) Watts, J. D.; Gauss, J.; Bartlett, R. J. Coupled-Cluster Methods with Non-iterative Triple Excitations for Restricted Open-Shell Hartree-Fock and Other General Single-Determinant Reference Functions. Energies and Analytical Gradients. *J. Chem. Phys.* **1993**, *98*, 8718−8733.
(36) Douglas, M.; Kroll, N. M. Quantum Electrodynamical Corrections to the Fine Structure of Helium. *Ann. Phys.* **1974**, *82*, 89−155.
(37) Jansen, G.; Hess, B. A. Revision of the Douglas-Kroll Transformation. *Phys. Rev. A* **1989**, *39*, 6016.
(38) Wolf, A.; Reiher, M.; Hess, B. A. The Generalized Douglas-Kroll Transformation. *J. Chem. Phys.* **2002**, *117*, 9215−9226.
(39) De Jong, W. A.; Harrison, R. J.; Dixon, D. A. Parallel Douglas−Kroll Energy and Gradients in NWChem: Estimating Scalar Relativistic Effects Using Douglas−Kroll Contracted Basis Sets. *J. Chem. Phys.* **2001**, *114*, 48−53.
(40) Purvis, G. D., III; Bartlett, R. J. A Full Coupled-Cluster Singles and Doubles Model: The Inclusion of Disconnected Triples. *J. Chem. Phys.* **1982**, *76*, 1910−1918.
(41) Raghavachari, K.; Trucks, G. W.; Pople, J. A.; Head-Gordon, M. A Fifth-order Perturbation Comparison of Electron Correlation Theories. *Chem. Phys. Lett.* **1989**, *157*, 479−483.
(42) Bartlett, R. J.; Musial, M. Coupled-Cluster Theory in Quantum Chemistry. *Rev. Mod. Phys.* **2007**, *79*, 291−352.
(43) Dixon, D. A.; Feller, D.; Peterson, K. A. A Practical Guide to Reliable First Principles Computational Thermochemistry Predictions Across the Periodic Table. In *Annual Reports in Computational Chemistry*, Wheeler, R. A.; Section, E. D.; Tschumper, G. S., Eds.; Elsevier: Amsterdam, 2012; Vol. *8*, pp 1−28.
(44) Feller, D.; Peterson, K. A.; Dixon, D. A. Further Benchmarks of a Composite, Convergent, Statistically-Calibrated Coupled Cluster-Based Approach for Thermochemical and Spectroscopic Studies. *Mol. Phys.* **2012**, *110*, 2381−2399.
(45) Peterson, K. A.; Feller, D.; Dixon, D. A. Chemical Accuracy in Ab Initio Thermochemistry and Spectroscopy: Current Strategies and Future Challenges. *Theor. Chem. Acc.* **2012**, *131*, No. 1079.
(46) Feller, D.; Peterson, K. A.; Dixon, D. A. The Impact of Larger Basis Sets and Explicitly Correlated Coupled Cluster Theory on the Feller-Peterson-Dixon Composite Method. In *Annual Reports in Computational Chemistry*; Elsevier: Dixon, 2016; Vol. *12*, pp 47−78.
(47) Dunham, J. L. The Energy Levels of a Rotating Vibrator. *Phys. Rev.* **1932**, *41*, 721−731.
(48) Gomes, A. S. P.; Saue, T.; Visscher, L.; Jensen, H. J. Aa.; Bast, R. *DIRAC, a Relativistic Ab Initio Electronic Structure Program, Release DIRAC19, 2019)*, 2022. http://www.diracprogram.org.
(49) Pyykkö, P.; Zhao, L.-B. Search for Effective Local Model Potentials for Simulation of Electrodynamic Effects in Relativistic Calculations. *J. Phys. B* **2003**, *36*, 1469−1478.
(50) Kállay, M.; Nagy, P. R.; Mester, D.; Gyevi-Nagy, L.; Csóka, J.; Szabó, P. B.; Rolik, Z.; Samu, G.; Csontos, J.; Hégely, B.et al.*MRCC, A Quantum Chemical Program Suite*; Budapest University of Technology and Economics: Budapest, 2022. www.mrcc.hu.
(51) Kállay, M.; Nagy, P. R.; Mester, D.; Rolik, Z.; Samu, G.; Csontos, J.; Csóka, J.; Szabó, P. B.; Gyevi-Nagy, L.; Hégely, B.; et al. The MRCC Program System: Accurate Quantum Chemistry from Water to Proteins. *J. Chem. Phys.* **2020**, *152*, No. 074107.
(52) Watts, J. D.; Bartlett, R. J. The Coupled-Cluster Single, Double, and Triple Excitation Model for Open-Shell Single Reference Functions. *J. Chem. Phys.* **1990**, *93*, 6104−6105.
(53) Noga, J.; Bartlett, R. J. The Full CCSDT Model for Molecular Electronic Structure. *J. Chem. Phys.* **1987**, *86*, 7041−7050.
(54) Kucharski, S. A.; Bartlett, R. J. Noniterative Energy Corrections through Fifth-Order to the Coupled Cluster Singles and Doubles Method. *J. Chem. Phys.* **1998**, *108*, 5243−5254.
(55) Reed, A. E.; Curtiss, L. A.; Weinhold, F. Intermolecular Interactions from a Natural Bond Orbital, Donor-Acceptor Viewpoint. *Chem. Rev.* **1988**, *88*, 899−926.
(56) Weinhold, F.; Landis, C. R. *Valency and Bonding: A Natural Bond Orbital Donor-Acceptor Perspective*; University Press: Cambridge, U.K., 2005.
(57) Glendening, E. D.; Landis, C. R.; Weinhold, F. NBO 7.0: New Vistas in Localized and Delocalized Chemical Bonding Theory. *J. Comput. Chem.* **2019**, *40*, 2234−2241.
(58) Glendening, E. D.; Badenhoop, J. K.; Reed, A. E.; Carpenter, J. E.; Bohmann, J. A.; Morales, C. M.; Karafiloglou, P.; Landis, C. R.; Weinhold, F. *Natural Bond Order 7.0*; Theoretical Chemistry Institute, University of Wisconsin: Madison, WI, 2018.
(59) Waldek, A.; Erdmann, N.; Grüning, C.; Huber, G.; Kunz, P.; Kratz, J. V.; Lassen, J.; Passler, G.; Trautman, N. RIMS Measurements

https://doi.org/10.1021/acs.jpca.2c06978
J. Phys. Chem. A 2022, 126, 9392−9407

for the Determination of the First Ionization Potential of the Actinides Actinium up to Einsteinium. *AIP Conf. Proc.* **2001**, *584*, 219−224.
(60) Scheer, M.; Bilodeau, R. C.; Brodie, C. A.; Haugen, H. K. Systematic Study of the Stable Sates of C^-, Si^-, Ge^-, and Sn^- Via Infrared Laser Spectroscopy. *Phys. Rev. A* **1998**, *58*, 2844−2856.
(61) Sansonetti, J. E.; Martin, W. C. Handbook of Basic Atomic Spectroscopic Data. *J. Phys. Chem. Ref. Data* **2005**, *34*, 1559−2259.
(62) Sevy, A.; Matthew, D. J.; Morse, M. D. Bond Dissociation Energies of TiC, ZrC, HfC, ThC, NbC and TaC. *J. Chem. Phys.* **2018**, *149*, No. 044306.
(63) Ruscic, B.; Pinzon, R. E.; Morton, M. L.; von Laszewski, G.; Bittner, S.; Nijsure, S. G.; Amin, K. A.; Minkoff, M.; Wagner, A. F. Introduction to Active Thermochemical Tables: Several "Key" Enthalpies of Formation Revisited. *J. Phys. Chem. A* **2004**, *108*, 9979−9997.
(64) Changala, P. B.; Nguyen, T. L.; Baraban, J. H.; Ellison, G. B.; Stanton, J. F.; Bross, D. H.; Ruscic, B. Active Thermochemical Tables: The Adiabatic Ionization Energy of Hydrogen Peroxide. *J. Phys. Chem. A* **2017**, *121*, 8799−8806.
(65) Argonne National Laboratory. Active Thermochemical Tables. https://atct.anl.gov/ThermochemicalData/version1.122g/index.php (accessed January 18, 2021).
(66) Curtiss, L. A.; Raghavachari, K.; Redfern, P. C.; Pople, J. A. Assessment of Gaussian-2 and Density Functional Theories for the Computation of Enthalpies of Formation. *J. Chem. Phys.* **1997**, *106*, 1063−1079.
(67) Wagman, D. D.; Evans, W. H.; Parker, V. B.; Schumm, R. H.; Halow, I.; Bailey, S. M.; Churney, K. L.; Nuttall, R. L. The NBS Tables of Chemical Thermodynamic Properties. Selected Values for Inorganic and C_1 and C_2 Organic Substances in SI units. *J. Phys. Chem. Ref. Data* **1982**, *18*, 1807−1812.
(68) Heaven, M. C.; Goncharov, V.; Steimle, T. C.; Ma, T.; Linton, C. The Permanent Electric Dipole Moments and Magnetic g Factors of UO. *J. Chem. Phys.* **2006**, *125*, No. 204314.
(69) Han, J.; Kaledin, L. A.; Goncharov, V.; Komissarov, A. V.; Heaven, M. C. Accurate Ionization Potentials for UO and UO_2: A Rigorous Test of Relativistic Quantum Chemistry Calculations. *J. Am. Chem. Soc.* **2003**, *125*, 7176−7177.
(70) Antonov, I. O.; Heaven, M. C. Spectroscopic and Theoretical Investigations of UF and UF^+. *J. Phys. Chem. A* **2013**, *117*, 9684−9694.
(71) Bross, D. H.; Peterson, K. A. Theoretical Spectroscopy Study of the Low-Lying Electronic States of UX and UX^+, X = F and Cl. *J. Chem. Phys.* **2015**, *143*, No. 184313.
(72) Li, W.-L.; Hu, H.-S.; Jian, T.; Lopez, G. V.; Su, J.; Li, J.; Wang, L.-S. Probing the Electronic Structures of Low Oxidation-State Uranium Fluoride Molecules UF_x^- (x = 2−4). *J. Chem. Phys.* **2013**, *139*, No. 244303.
(73) de Melo, G.; Vasiliu, M.; Marshall, M.; Zhu, Z.; Tufekci, B. A.; Bowen, K. H.; Dixon, D. A. The Interaction of H and H^- with U from an Experimental and Computational Perspective. *J. Phys. Chem. A* **2022**, *126*, 4432−4443.
(74) Pyykkö, P. Additive Covalent Radii for Single-, Double-, and Triple-Bonded Molecules and Tetrahedrally Bonded Crystals: A Summary. *J. Phys. Chem. A* **2015**, *119*, 2326−2337.

https://doi.org/10.1021/acs.jpca.2c06978
J. Phys. Chem. A 2022, 126, 9392−9407